Energy Policy 220 (2027) 115646

Contents lists available at ScienceDirect

Energy Policy

journal homepage: www.elsevier.com/locate/jepo

Modeling optimal incentives for the electric vehicle market

Paul Vincent Johnson [a,*], Dávid Zoltán Szabó [b]

[a] Department of Mathematics, The University of Manchester, Oxford Rd, Manchester, M13 9PL, United Kingdom
[b] Corvinus, University of Budapest, Fővám tér 13-15, Budapest, 1093, Hungary

HIGHLIGHTS

- In the UK model, around 12.8 million ICE cars remain in 2050 absent intervention.
- Terminal and sales-based penalties imply distinct policy timing paths.
- Fuel-tax dependence weakens optimal electrification incentives.
- Higher demand responsiveness improves policy cost-effectiveness.
- Results indicate fiscal reform can materially facilitate the EV transition.

ARTICLE INFO

Keywords:
Electric vehicles
Transport decarbonization
Fiscal policy
Fuel taxation
Policy timing
Fleet dynamics

ABSTRACT

Governments face increasing pressure to meet legally binding net-zero targets, requiring a rapid transition from internal combustion engine (ICE) vehicles to electric vehicles (EVs). Designing effective incentive schemes is challenging because vehicle fleets adjust slowly, policy interventions are fiscally costly, and electrification erodes fuel-tax revenues.

This paper develops a dynamic policy evaluation framework that combines cross-country evidence on EV adoption with long-run fleet dynamics under uncertainty. Using both the United Kingdom and France as case studies, we simulate optimal time paths of EV purchase incentives under alternative policy objectives, including terminal fleet targets, sales-based penalties, and fiscal revenue considerations.

The results reveal three core findings. First, stock-based (terminal) penalties may delay intervention but strongly stabilize long-run fleet outcomes, while sales-based penalties induce earlier but less targeted action. Second, dependence on fuel-tax revenues creates a fiscal lock-in mechanism that weakens optimal electrification incentives. Third, the effectiveness of subsidy programs depends critically on consumer responsiveness to price incentives.

Overall, the analysis shows that EV transition policy is best evaluated jointly with fiscal reform and long-run fleet dynamics. Well-timed and fiscally coherent intervention can substantially reduce emissions while limiting long-term budgetary risks.

1. Introduction

Decarbonizing road transport is central to achieving national net zero commitments. Passenger vehicles account for a substantial share of transport-related CO_2 emissions, and many advanced economies have announced phase-out dates for new internal combustion engine (ICE) vehicles between 2030 and 2040. Achieving these targets requires not only technological progress but also carefully timed public intervention, as vehicle fleets adjust slowly and capital turnover occurs over decades.

The gradual nature of fleet renewal creates a dynamic policy challenge. Changes in new vehicle sales translate only gradually into changes in the stock of vehicles on the road. Early intervention accelerates decarbonization but entails sustained fiscal expenditure, while delayed intervention risks costly policy adjustments as climate deadlines approach. In addition, electrification reduces fuel-tax revenues, introducing fiscal feedback effects that interact with environmental objectives.

This paper develops a dynamic policy evaluation framework to study the optimal timing of electric vehicle (EV) incentives under uncertainty. We combine cross-country data on EV sales shares, vehicle prices, public

* Corresponding author.
Email address: paul.johnson-2@manchester.ac.uk (P.V. Johnson).

https://doi.org/10.1016/j.enpol.2026.115646
Received 17 March 2026; Received in revised form 28 September 2026; Accepted 29 September 2026
Available online 8 October 2026
0301-4215/© 2026 The Author(s). Published by Elsevier Ltd. This is an open access article under the CC BY license (http://creativecommons.org/licenses/by/4.0/).

incentives, and charging infrastructure with a structural model of fleet dynamics and government decision-making. Rather than pursuing causal econometric identification, the empirical component serves as a data-driven calibration. It anchors a reduced-form EV adoption function in realistic magnitudes, which is then embedded into a stochastic optimal control framework governing the evolution of the vehicle fleet.

The government is modeled as choosing a time path of purchase incentives to minimize discounted fiscal costs associated with the transition. To ensure policy interpretability, the objective function is explicitly mapped to three observable policy dimensions: (i) a terminal cost representing the shadow value of failing to meet a legally binding long-run emissions or fleet-composition target; (ii) a flow cost associated with ongoing ICE sales, corresponding to sales standards or feebate-type schemes; and (iii) the fiscal opportunity cost of declining fuel-tax revenues as electrification progresses. These components allow alternative policy environments to be evaluated within a unified framework.

Consistent with empirical evidence that consumers do not fully internalize long-run operating costs when making vehicle purchase decisions, the demand specification separates upfront purchase incentives from longer-term fiscal revenue streams. This modeling choice allows the government's intertemporal fiscal trade-offs to be analyzed transparently without imposing strong assumptions about perfect foresight or full cost internalization by households.

Uncertainty in EV prices is introduced through a stochastic process, allowing optimal policy to respond dynamically to realized market conditions. Using the United Kingdom as our main case study, we simulate optimal incentive paths under alternative policy objectives and quantify their fiscal and fleet-composition implications through 2050.

The contribution of the paper is to integrate observed incentive structures with long-horizon fleet dynamics in a transparent and policy-interpretable framework. By explicitly modeling the interaction between sales flows, stock evolution, fiscal revenues, and uncertainty, the analysis clarifies how different policy objectives translate into distinct optimal timing strategies. The modeling framework is designed to be transferable across countries, subject to country-specific recalibration of fleet dynamics, prices, incentives, adoption conditions, and fiscal parameters. To demonstrate this, we apply the framework to France as a robustness exercise and examine how the resulting optimal strategy differs from the UK calibration.

The remainder of the paper proceeds as follows. Section 2 reviews the related literature. Section 3 introduces the fleet dynamics and demand framework. Section 4 describes the empirical calibration. Section 5 presents numerical results under alternative policy environments. Section 6 concludes.

2. Related literature

This paper relates to several strands of literature on EV adoption, transport decarbonization policy, and dynamic technology transition.

A large empirical literature studies the determinants of EV adoption and the effectiveness of financial incentives. Survey-based and discrete choice studies highlight the role of vehicle prices, range, and charging infrastructure in shaping consumer preferences (Liao et al., 2017; Shepherd et al., 2012). More recent quasi-experimental evidence shows that purchase subsidies and tax credits significantly increase EV uptake, although effects vary across income groups and local market conditions (Muehlegger and Rapson, 2022; He et al., 2023). Reviews such as Hardman et al. (2017) and Anilan and Vij (2024) conclude that financial incentives are generally effective but subject to heterogeneity and diminishing returns.

Furthermore, structural models in industrial organization emphasize endogenous pricing, indirect network effects of charging infrastructure, and substitution patterns among EVs and different ICE segments (Springel, 2021; Xing et al., 2021; Remmy, 2026). These studies provide detailed micro-level insights into demand and firm behavior. Unlike this micro-structural literature, we do not estimate short-run causal effects or endogenous pricing responses; instead, we use observed aggregate adoption patterns to discipline a macro-level, long-horizon dynamic framework.

A related body of work analyzes EV diffusion and fleet transition dynamics. Classical diffusion models such as the Bass model (Bass, 1969) have been widely applied to vehicle markets (Massiani and Gohs, 2015). More recent contributions incorporate infrastructure constraints, social spillovers, and dynamic feedback mechanisms (Feng et al., 2019; Javid and Nejat, 2017). Scenario-based projections show that fleet turnover is inherently slow and that changes in new sales translate only gradually into emissions reductions (Rietmann et al., 2020; International Energy Agency, 2024). Our framework builds directly on this insight by modeling the interaction between sales flows, retirement rates, and long-run stock outcomes.

A third strand of literature evaluates the cost competitiveness of EVs relative to ICE vehicles. Numerous studies document declining battery costs and narrowing total cost of ownership gaps (Liu et al., 2021; Burnham et al., 2021; Slowik et al., 2022). However, substantial heterogeneity across vehicle classes and tax regimes remains (Mitropoulos and Prevedouros, 2017). These cost dynamics motivate continued policy intervention and provide key inputs into our calibration.

From a policy perspective, research on carbon taxation and fuel taxation highlights the central role of transport taxes in climate policy (Sterner, 2007; Bretschger and Grieg, 2024). Broader analyses examine how carbon pricing interacts with existing fiscal systems and distortionary taxation (Metcalf, 2007; Goulder, 2013; OECD, 2021). In parallel, work on directed technical change emphasizes the importance of credible long-term signals for sustaining low-carbon innovation (Acemoglu et al., 2012; Aghion et al., 2016). Our contribution complements this literature by focusing specifically on fleet-level dynamics and the timing of incentives under binding long-run targets.

Finally, a growing theoretical literature studies dynamic green investment and policy design under uncertainty (Basei et al., 2024; Flora and Tankov, 2023; Szabó et al., 2025). While these models provide valuable conceptual insights, they typically abstract from empirically grounded fleet structures and observed incentive regimes. We contribute by integrating real-world incentive data with a stochastic optimal control framework that captures fiscal trade-offs and gradual capital turnover.

Overall, the paper bridges empirical evidence on EV incentives with dynamic policy evaluation, focusing on how alternative objective structures translate into distinct optimal timing strategies over multi-decade horizons.

3. Model

This section presents the dynamic framework describing the transition of a national passenger car fleet from internal combustion engine (ICE) vehicles to electric vehicles (EVs). The model captures (i) total fleet dynamics, (ii) the split between ICE and EV stocks, (iii) EV adoption behavior, and (iv) the government's intertemporal policy problem. The focus is on transparency and economic interpretation rather than analytical generality.

3.1. Total fleet dynamics

Let $n(t)$ denote the total number of passenger vehicles in use at time t. In mature economies, the number of cars per capita has remained relatively stable over time (van Dender and Clever, 2013; Goodwin, 2020; Eurostat, 2025). We therefore assume that fleet size is proportional to population:

$$n(t) = \Gamma P(t), \tag{1}$$

where $P(t)$ is population and Γ is a country-specific fleet-to-population scaling coefficient.

Fleet dynamics are governed by new vehicle sales $v_s(t)$ and retirements $v_r(t)$:

$$\frac{dn(t)}{dt} = v_s(t) - v_r(t). \tag{2}$$

Vehicle retirements depend on the expected retirement age $T_r(t)$, which we model as gradually adjusting over time to reflect technological durability improvements and regulatory developments:

$$T_r(t) = T_0 + \frac{T_\infty - T_0}{1 + e^{-\gamma_r(t-t_r)}}. \tag{3}$$

This specification captures a smooth transition from the current retirement age T_0 toward a long-run level T_∞.

To connect sales, retirements, and fleet size in a tractable way, we approximate the age distribution of vehicles using a parametric representation consistent with observed average retirement ages. This yields closed-form expressions linking $v_s(t)$ and $v_r(t)$ to $n(t)$ and $T_r(t)$. The full derivation is provided in Appendix C.

Intuitively, higher retirement ages mechanically slow fleet turnover, increasing the persistence of existing ICE vehicles even if new sales shift rapidly toward EVs.

3.2. ICE and EV stocks

Let $m(t)$ denote the stock of ICE vehicles and let $p(t) = n(t) - m(t)$ denote the stock of EVs. The EV sales share is denoted by $\lambda(t)$, so that EV and ICE sales satisfy

$$\phi_s(t) = \lambda(t)v_s(t), \qquad \mu_s(t) = (1 - \lambda(t))v_s(t). \tag{4}$$

The ICE stock evolves according to

$$\frac{dm(t)}{dt} = \mu_s(t) - \mu_r(t), \tag{5}$$

where $\mu_r(t)$ denotes ICE retirements.

Retirements are proportional to total fleet retirements but are weighted by the relative age structure of ICE vehicles. This ensures that older ICE fleets retire faster, while retirements remain bounded between zero and total fleet retirements. The exact functional form used for numerical implementation is provided in Appendix C.

The key implication is structural inertia: even if EV sales rapidly increase, the ICE stock declines only gradually because retirement dynamics depend on past sales.

3.3. EV adoption

The EV sales share follows a logistic specification:

$$\ln\left(\frac{\lambda(t)}{1-\lambda(t)}\right) = \beta_0 + \delta_c + \beta_1 \ln\left(\frac{P_{\mathrm{EV}}(t)}{P_{\mathrm{ICE}}(t)}\right) + \beta_2 \ln\left(1 - \frac{\pi(t)}{P_{\mathrm{EV}}(t)}\right) + \beta_3 \ln C_p(t), \tag{6}$$

where P_{EV} and P_{ICE} denote average purchase prices, $\pi(t)$ is the EV purchase incentive, and $C_p(t)$ measures charging infrastructure availability.

The coefficients $(\beta_0, \beta_1, \beta_2, \beta_3)$ are estimated using cross-country data and serve as calibration inputs rather than structural demand parameters. For country-specific dynamic simulations, δ_c is a constant adoption adjustment chosen to match the observed EV sales share at observed vehicle prices, incentives and charging infrastructure in a reference year. The adjustment is a calibration residual, not a separately estimated causal country effect. It is held fixed within each simulation scenario.

The pooled regressions reported in Section 4 estimate the specification without δ_c. The country adjustment is introduced subsequently when calibrating the dynamic model. EV prices follow an exogenous downward trend reflecting technological progress, with stochastic deviations capturing uncertainty in battery costs:

$$dz(t) = -\kappa z(t)\,dt + \sigma dW(t). \tag{7}$$

ICE prices and charging infrastructure follow deterministic growth paths. These assumptions abstract from endogenous pricing and two-sided market feedbacks, allowing us to focus on policy timing rather than industrial organization dynamics.

3.4. Government problem

The government chooses the incentive path $\pi(t)$ to minimize the discounted fiscal cost of the transition, subject to fleet inertia.

The objective function consists of three components:

- **Terminal target penalty (K_1):** The shadow cost of failing to meet a long-run climate mandate, applied to the remaining ICE stock at horizon T.
- **Flow/sales penalty (K_2):** A per-unit cost associated with ongoing ICE sales, conceptually equivalent to emissions standards or feebate schemes.
- **Fiscal opportunity cost (K_3):** The loss of fuel-tax revenues generated by ICE vehicles.

While the government internalizes the long-run fiscal impact of fuel taxes, we assume consumers are myopic with respect to future operating costs at the time of purchase, consistent with evidence on the energy efficiency gap (Gillingham et al., 2021). Thus, usage taxes affect the government's objective but do not directly enter the EV adoption equation.

The government minimizes

$$\min_{\pi} \mathbb{E}\left[\int_{t_0}^{T} \left(\lambda v_s \pi + (1-\lambda)v_s K_2 + mK_3\right) e^{-r(t-t_0)} dt + m(T)K_1 e^{-r(T-t_0)}\right]. \tag{8}$$

This defines a stochastic optimal control problem with state variables given by EV cost uncertainty and fleet composition. The associated Hamilton–Jacobi–Bellman equation and numerical solution procedure are presented in Appendix E.

The framework highlights how policy timing interacts with structural fleet inertia, fiscal feedback effects, and uncertainty in technological progress.

4. Empirical investigation

The empirical implementation serves two purposes. First, we estimate the reduced-form EV sales-share function introduced in Eq. (6) using cross-country panel data. Second, we calibrate the fleet block of the model to the United Kingdom (and later France) in order to simulate long term transition pathways under alternative policy environments.

The empirical component is not intended to provide structural identification of demand parameters. Instead, it provides empirically grounded magnitudes that discipline the dynamic policy framework. More details on how the data were collected and processed for the cross-country calibration are documented in Appendix B, while information on the country-specific calibrations is provided in Appendix D.

4.1. Estimation of the EV adoption function

We estimate the EV sales-share function using a balanced panel of 14 countries over 2021–2024. The sample includes the United Kingdom, France, Germany, Spain, Sweden, Norway, the Netherlands, Italy, China, Brazil, Indonesia, Mexico, India, and the United States.

Data on EV sales shares and charging infrastructure are obtained from the International Energy Agency's *Global EV Data Explorer* (International Energy Agency (IEA), 2025). Country-level purchase

incentives and sales-weighted vehicle prices are constructed from official government publications and industry sources, as detailed in Appendix B. All monetary values are converted to USD using annual average exchange rates.

Table 1 reports EV sales shares. Adoption differs substantially across countries. Norway exceeds 90% EV share by 2024, while several emerging economies remain below 10%. China exhibits rapid growth, and several European markets display volatility following changes in incentive schemes.

Table 2 presents sales-weighted average manufacturer's suggested retail prices (MSRP) for ICE and EV vehicles. In most countries, EVs remain more expensive on average, partly reflecting segment composition. China is an exception, where domestic production narrows the EV–ICE price differential. Because the demand specification depends on relative prices, currency denomination does not affect the estimation results.

Table 3 reports the harmonized average public incentive per EV sold. This measure aggregates direct purchase grants, tax exemptions, registration fees, circulation tax advantages, and benefit-in-kind provisions into a comparable upfront equivalent. Recurring tax advantages are converted into present values using a constant discount rate. Fuel tax advantages are excluded and instead enter the government's objective separately.

Table 1
Market share λ of EVs (BEV and PHEV) by Country (2021–2024).

Country	2021	2022	2023	2024
UK	19.0%	23.0%	24.0%	28.0%
France	17.0%	20.0%	25.0%	24.0%
Germany	26.0%	31.0%	24.0%	19.0%
Spain	7.3%	8.9%	12.0%	11.0%
Sweden	43.0%	54.0%	60.0%	58.0%
Norway	86.0%	89.0%	90.0%	92.0%
Netherlands	29.0%	35.0%	44.0%	48.0%
Italy	9.1%	8.5%	9.2%	7.9%
China	15.0%	29.0%	38.0%	48.0%
Brazil	0.9%	1.2%	3.0%	6.4%
Indonesia	0.1%	1.4%	2.2%	7.3%
Mexico	0.8%	1.0%	1.5%	2.2%
India	0.4%	1.4%	2.1%	2.1%
USA	4.7%	7.4%	9.5%	10.0%

Table 2
Sales-weighted average MSRP in USD, by Country and Power Train (2021–2024). When official sales-weighted averages are unavailable, MSRPs are reconstructed using manufacturer list prices or transaction prices reported in industry publications. In particular, where official sales-weighted price data were unavailable for Indonesia and Mexico, approximate ICE-price estimates were constructed from available market and industry sources. These estimates are rounded to the nearest thousand USD to reflect the lower precision of the underlying source information and should not be interpreted as exact sales-weighted averages. Original currencies are converted to USD using an average exchange rate for the given year.

	ICE MSRP (USD)				EV MSRP (USD)			
Country	2021	2022	2023	2024	2021	2022	2023	2024
UK	34,681	32,576	34,711	37,778	52,936	49,684	53,082	60,074
France	32,953	31,652	33,894	33,644	52,045	46,969	48,034	50,704
Germany	46,396	47,778	51,486	49,915	61,487	57,271	59,767	59,388
Spain	32,953	31,652	33,894	33,644	55,529	50,424	51,929	55,320
Sweden	46,396	47,778	51,486	49,915	61,775	57,274	59,573	59,879
Norway	71,251	68,530	70,715	68,728	87,097	78,568	79,762	76,366
Netherlands	46,396	47,778	51,486	49,915	61,487	57,271	59,767	59,388
Italy	32,953	31,652	33,894	33,644	52,045	46,969	48,034	50,704
China	27,633	28,482	28,556	29,334	29,165	28,143	26,652	26,206
Brazil	23,584	26,775	28,033	26,082	82,391	74,339	68,448	36,638
Indonesia	20,000	20,000	20,000	20,000	53,000	53,000	57,256	45,410
Mexico	20,000	23,000	26,000	29,000	55,260	61,400	67,540	59,918
India	14,086	15,217	15,272	15,588	30,383	28,609	25,494	23,648
USA	40,315	44,315	47,105	46,105	54,595	64,544	57,763	57,257

Charging infrastructure density, measured as public charging points per million inhabitants, is reported in Table 4. Western European countries exhibit consistently higher infrastructure density than emerging economies. It is important to note that the seemingly high incentive values for emerging economies such as Brazil and Indonesia do not represent direct cash transfers. These values reflect the financial equivalent of exemptions from otherwise high import tariffs and luxury vehicle taxes, which mechanically translate into large modeled EV–ICE price differentials in USD terms.

The EV sales-share function is estimated according to Eq. (6). For this pooled estimation, the country-specific calibration adjustment δ_c is omitted. The estimated coefficients are subsequently combined with a country-specific adoption anchor for the dynamic simulations. Explanatory variables include the EV–ICE price ratio, the net-of-subsidy EV price term, and charging infrastructure availability.

Table 5 reports three nested beta regression specifications. Model 1 includes only the relative price variable and indicates a statistically significant negative association between the EV price premium and adoption. Model 2 adds the incentive variable, which substantially improves model fit according to log-likelihood, AIC, and BIC criteria. Model 3 incorporates charging infrastructure and provides the strongest overall fit.

The estimated coefficient on the incentive term is large in magnitude relative to the price differential term, indicating that fiscal incentives contribute materially to explaining cross-country variation in EV adoption. Charging infrastructure enters positively and significantly, though with a smaller marginal effect.

Variance Inflation Factor statistics suggest moderate correlation among regressors but no evidence of severe multicollinearity. Given

Table 3
Average incentive π per EV car sold (BEV and PHEV) by country (2021–2024). Original currencies are converted to USD using the average exchange rate for the given year.

Country	2021	2022	2023	2024
UK	12,805	12,141	11,883	13,008
France	12,213	10,402	9336	8211
Germany	8899	8068	6016	3384
Spain	9637	8669	10,594	12,347
Sweden	9752	9609	5992	6160
Norway	31,731	28,570	25,669	26,255
Netherlands	10,900	8600	8700	8500
Italy	8270	6789	6823	6816
China	4867	4239	2964	3803
Brazil	24,934	22,925	21,455	8750
Indonesia	4250	14,000	20,250	19,410
Mexico	11,870	13,010	14,150	11,528
India	9411	9040	7149	6312
USA	7492	7645	3621	3851

Table 4
Public charging points per million people by country (2021–2024).

Country	2021	2022	2023	2024
UK	510.37	761.76	1052.63	1279.07
France	829.17	1368.42	1781.14	2264.58
Germany	715.28	1036.14	1325.30	1894.46
Spain	176.60	259.23	542.37	867.02
Sweden	1317.31	1676.19	3566.04	4168.22
Norway	3581.82	4545.45	5090.91	5636.36
Netherlands	4788.57	7073.86	8192.09	10,561.80
Italy	368.77	631.00	801.67	1001.67
China	813.55	1246.46	1914.89	2485.23
Brazil	4.30	14.60	21.90	57.60
Indonesia	0.70	2.20	3.80	11.40
Mexico	9.70	11.70	12.20	14.00
India	3.52	7.74	26.03	52.26
USA	339.64	385.07	474.48	569.32

Table 5
Results of Beta Regression models Predicting EV sales Share. Coefficient estimates for main predictors are in **bold**. $^{***}p < 0.01$, $^{**}p < 0.05$, $^{*}p < 0.10$.

Variable	Model 1 $\ln \frac{\lambda}{1-\lambda} \sim x_1$	Model 2 $\ln \frac{\lambda}{1-\lambda} \sim x_1 + x_2$	Model 3 $\ln \frac{\lambda}{1-\lambda} \sim x_1 + x_2 + x_3$
β_0	0.000	−0.829***	−5.509***
	(0.207)	(0.240)	(0.529)
β_1 (x_1)	**−2.910*****	**−4.339*****	**−2.056*****
	(0.480)	(0.503)	(0.471)
β_2 (x_2)		**−5.262*****	**−6.457*****
		(0.957)	(0.695)
β_3 (x_3)			**0.538*****
			(0.059)
Precision Model			
ϕ	1.546***	2.109***	3.284***
	(0.193)	(0.204)	(0.204)
Fit Statistics			
No. Observations	56	56	56
Log-Likelihood	46.5	57.9	83.6
AIC	−87.1	−107.8	−157.3
BIC	−81.0	−99.7	−147.2

the short time dimension and aggregate nature of the data, the estimates should be interpreted as reduced-form relationships capturing cross-country variation rather than structural demand elasticities.

The relative price coefficient remains negative and statistically significant across specifications, including fractional logit models with country and year fixed effects. This stability supports its use as a calibration input in the dynamic policy model. Robustness checks using fractional logit estimators following Papke and Wooldridge (1996) are reported in Appendix A.

4.2. Fuel taxation and fiscal calibration

ICE vehicles generate substantial public revenue through fuel duties and carbon-related taxation. While ownership-based taxes are incorporated in the incentive variable, fuel duty affects vehicle usage and is therefore treated separately in the model via parameter K_3 in Eq. (8).

This separation is consistent with the literature emphasizing the distinct economic roles of ownership and usage taxes in transport demand (Sterner, 2007; Bretschger and Grieg, 2024).

For the United Kingdom, fuel duty is calibrated using statutory rates and average driving behavior. Because the model horizon extends to 2050, the calibration uses the long-run main fuel-duty rate of £0.5795 per litre which is the statutory rate legislated to apply from March 2027, once the temporary 5 pence per litre reduction in force since March 2022 (a reduced rate of £0.5295) is fully unwound (HM Revenue & Customs, 2026). Together with the 20% VAT attributable to the duty component, an average annual mileage of approximately 7100 miles and fuel consumption of 7 L per 100 km, the implied annual tax revenue per ICE vehicle is approximately

$$K_3 = -\left(7{,}100 \times 1.609344 \times \frac{7}{100} \times 0.5795 \times 1.20\right) \approx -556.21.$$

The negative sign reflects government revenue, which offsets expenditure in the objective through the term $K_3\,\mathrm{m}(t)$. The calculation includes fuel duty and VAT attributable to the duty component, rather than VAT on the full pump price. Simulations use the unrounded calculated value, $K_3 = -556.211495$; the displayed value is rounded to the nearest penny.

4.3. United Kingdom calibration

The United Kingdom is used as a case study for dynamic simulation. It represents a mature vehicle market with a relatively stable cars-per-capita ratio and sustained investment in charging infrastructure.

Population projections are obtained from the UK Office for National Statistics (Office for National Statistics, 2025). A smooth quadratic approximation is fitted to projected values to generate a continuous population path. Fleet size is computed using Eq. (1). The scaling coefficient Γ is chosen (and then held constant) so that the resulting fleet path $n(t) = \Gamma P(t)$ coincides with the observed UK fleet at the simulation start time $t_0 = 2025$.

Observed registration and fleet-stock statistics over the period 2015–2024 are used to construct total vehicle sales and implied retirements. The retirement-age function is calibrated to match as closely as possible the observed turnover patterns, implying gradual increases in average vehicle lifetime consistent with recent trends.

Separately, parameters in the EV adoption equation are anchored to the 2024 market observation. Let $t_a = 2024$ denote the reference observation year and $t_0 = 2025$ the start of the policy simulations. Using observed EV sales share λ_a, vehicle prices $P_{\mathrm{EV},a}$ and $P_{\mathrm{ICE},a}$, incentive π_a, and charging density $C_{p,a}$, we set

$$\delta_{\mathrm{UK}} = \ln\left(\frac{\lambda_a}{1-\lambda_a}\right) - \beta_0 - \beta_1 \ln\left(\frac{P_{\mathrm{EV},a}}{P_{\mathrm{ICE},a}}\right) - \beta_2 \ln\left(1 - \frac{\pi_a}{P_{\mathrm{EV},a}}\right) - \beta_3 \ln C_{p,a}. \tag{9}$$

This ensures that the model implied adoption rates match the observed rate in 2024 taking the observed prices and incentive as inputs (see Tables 1–4 for UK 2025 data).

During the simulation period $t \geq t_0$, vehicle prices follow

$$P_{\mathrm{ICE}}(t) = P_{\mathrm{ICE},a} \exp\left[\theta_2 (t - t_a)\right], \tag{10}$$

$$P_{\mathrm{EV}}(t) = P_{\mathrm{EV},a} \exp\left[\theta_1 (t - t_a) + z(t) - z_0\right], \tag{11}$$

where $z(t_0) = z_0$ and $z(t)$ follows Eq. (7). Thus, at the simulation start, both prices are obtained from their observed reference-year values using their respective price trends. Subsequent mean reversion of $z(t)$ contributes to the EV price path.

Charging density follows

$$C_p(t) = C_{p,a} \exp\left[\theta_3 (t - t_a)\right].$$

These exogenous paths are specified independently of the estimated demand coefficients and the country adoption adjustment.

The no-intervention scenario sets $\pi(t) = 0$ during the simulation period. It therefore removes the modeled incentive rather than continuing the observed incentive π_a. Consequently, its initial projected EV sales share need not equal the observed reference-year share used for calibration.

Fig. 1 summarizes the resulting baseline projections. Under zero incentives, a substantial ICE stock remains in 2050. Even sustained high incentives reduce but do not eliminate the ICE fleet. These baseline simulations illustrate the structural inertia embedded in fleet dynamics and motivate the optimal policy analysis in the following section.

5. Results

This section presents the numerical results of the optimal control problem defined in Eq. (8), subject to the fleet dynamics (5) and the EV adoption Eq. (6).

All simulations use the United Kingdom calibration described in Section 4. Parameter values are taken directly from the empirical estimates and calibration assumptions reported in Sections 3 and 4, together with the numerical specifications detailed in Appendix E.

We address three central questions:

1. How does policy timing differ under stock-based versus flow-based penalties?
2. How do these instruments affect long-run fleet composition and cumulative emissions?
3. How does fuel taxation alter optimal intervention thresholds?

Stochastic results correspond to medians and interquartile ranges across Monte Carlo simulations of the EV price process defined in Eq. (7).

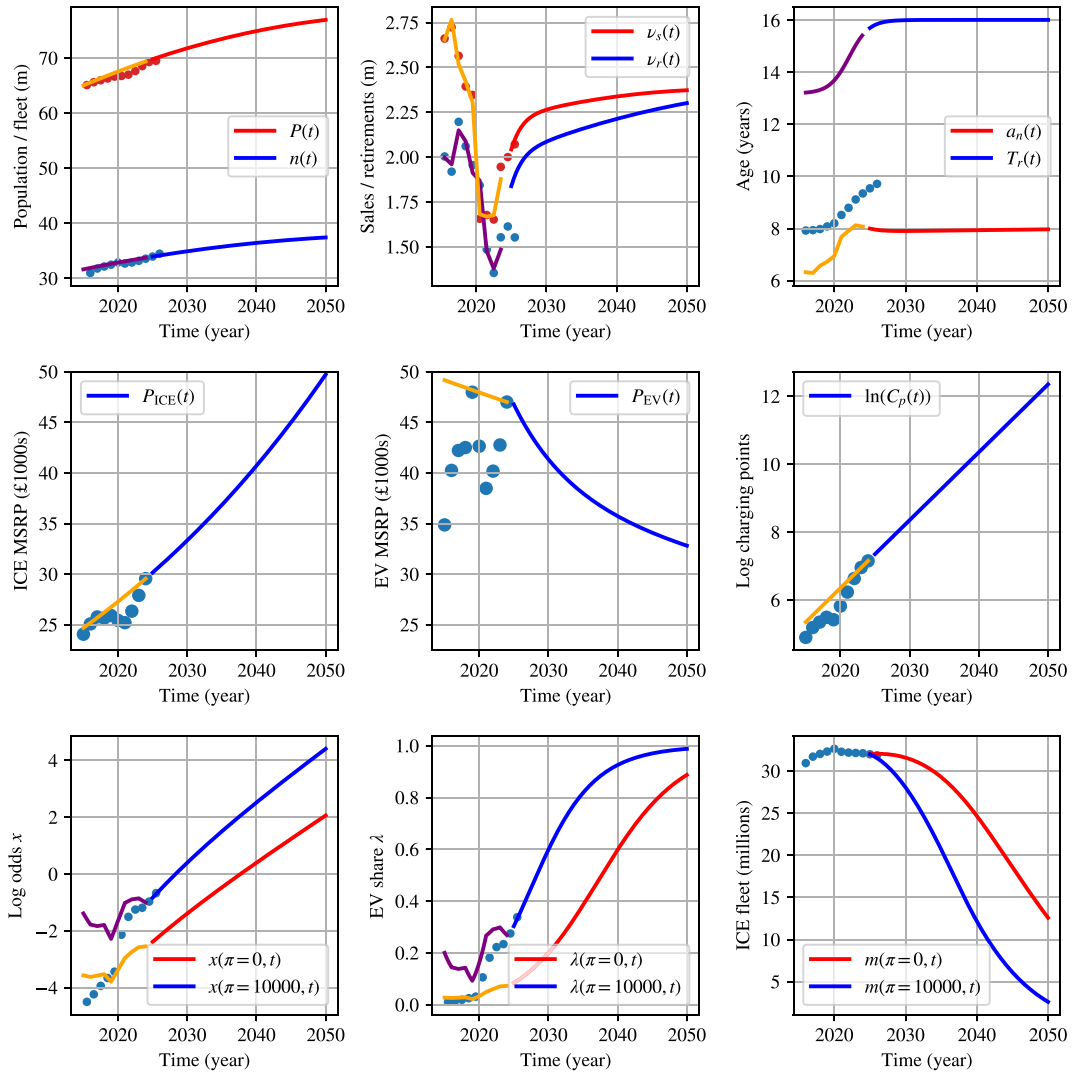


Fig. 1. This figure shows the projections for exogenous and endogenous variables as a function of time, alongside observed historical data points (blue and Orange dots) and model fits (Orange and purple lines). Here for projections we set $z_0 = 0.25$, $\kappa = 0.1$, $\theta_1 = -0.005$, $\theta_2 = 0.02$ and $\theta_3 = 0.2$. For demand and predicted number of ICE cars, we set a policy of $\pi = 0$ or $\pi = 10{,}000$ to show the possible variation in results. Vehicle prices are projected from observed 2024 values; the country-specific intercept adjustment matches observed 2024 adoption at the observed incentive. (For interpretation of the references to colour in this figure legend, the reader is referred to the web version of this article.)

5.1. Example strategies: Deterministic versus stochastic control

We begin by comparing optimal policies under deterministic and stochastic demand dynamics. The government minimizes the objective in Eq. (8), subject to fleet dynamics (5) and EV adoption behavior (6). Uncertainty enters through the EV price process defined in Eq. (7).

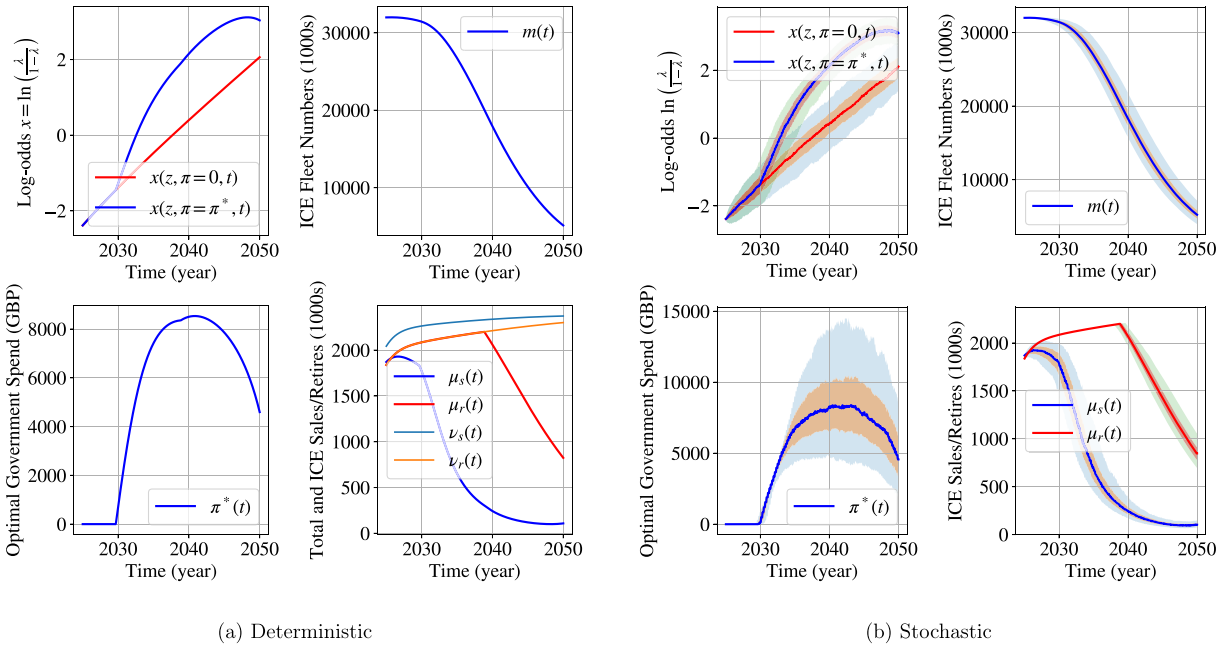
In the deterministic case ($\sigma = 0$), the problem reduces to the two-point boundary value system described in Appendix E. The optimal incentive path $\pi^*(t)$ is obtained from the first-order condition (E.7), together with the state and costate dynamics.

In the stochastic case ($\sigma > 0$), the Hamilton–Jacobi–Bellman equation is solved numerically using the dynamic programming scheme detailed in Appendix E. The resulting feedback policy $\pi^*(z, m, s_m, t)$ is then simulated forward over 500 Monte Carlo paths. Reported stochastic trajectories correspond to medians and interquartile ranges.

First we consider the results for a terminal penalty regime, with $K_1 = 100{,}000 > 0$ and $K_2 = K_3 = 0$. Fig. 2 shows that when policy costs enter exclusively through the terminal term $m(T)K_1$ in Eq. (8), the optimal strategy delays intervention. Incentives remain close to zero in the early part of the horizon and increase sharply only as the terminal date approaches. This pattern reflects intertemporal discounting: future penalties are discounted at rate r, reducing the value of early intervention when costs are concentrated at the horizon. Stated directly, the mechanism of a terminal-stock penalty is that it prices only the ICE vehicles still on the road at the horizon T; early sales patterns matter solely through their effect on that terminal stock, so the government optimally concentrates spending late, when it has the greatest leverage over the end-of-horizon fleet.

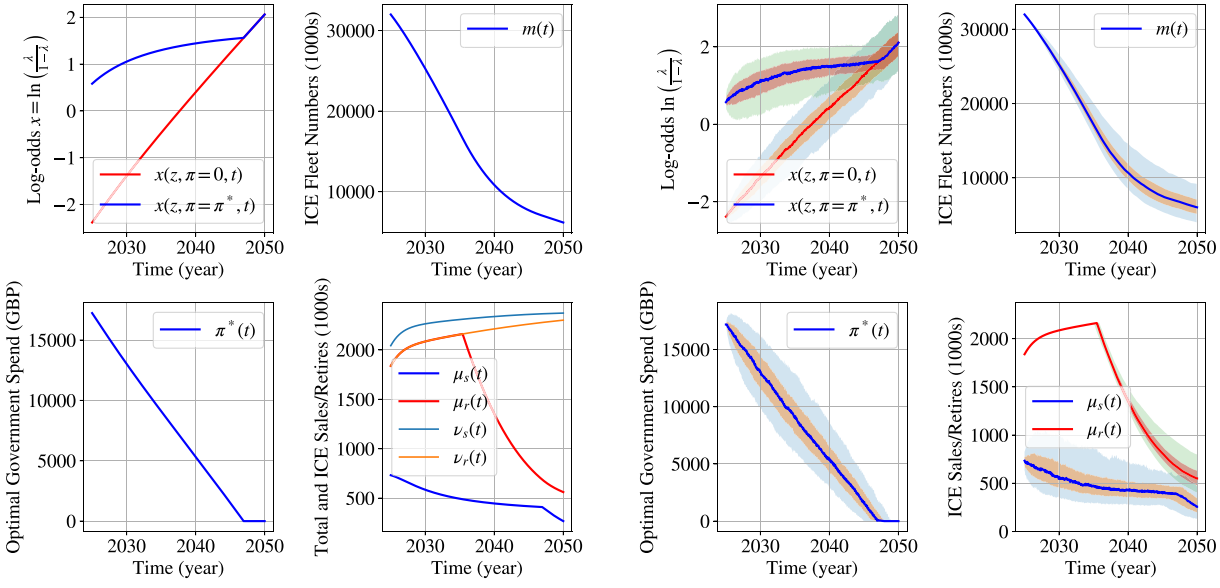
Under stochastic demand, the median incentive path closely tracks the deterministic benchmark. However, realized incentives fluctuate across simulation paths in response to shocks in the EV price process (7). When EV costs fall unexpectedly, incentives decline; when costs rise, incentives increase to maintain the desired fleet trajectory. Despite volatility in the policy instrument, dispersion in the final ICE stock remains limited, indicating that adaptive policy stabilizes long-run outcomes.

Next we examine a sales penalty regime with $K_2 = 30{,}000$ and other costs absent $K_1 = K_3 = 0$. In this case the penalties apply continuously to ICE sales through the term $(1 - \lambda)\nu_s K_2$ in Eq. (8), so the optimal incentives are introduced immediately and decline gradually over time.



(a) Deterministic (b) Stochastic

Fig. 2. Optimal incentive paths and fleet dynamics under a large terminal penalty ($K_1 = 100{,}000$, $K_2 = K_3 = 0$). Panel (a) reports the deterministic solution obtained via Pontryagin's Minimum Principle. Panel (b) reports the stochastic solution (median and interquartile range across Monte Carlo simulations).



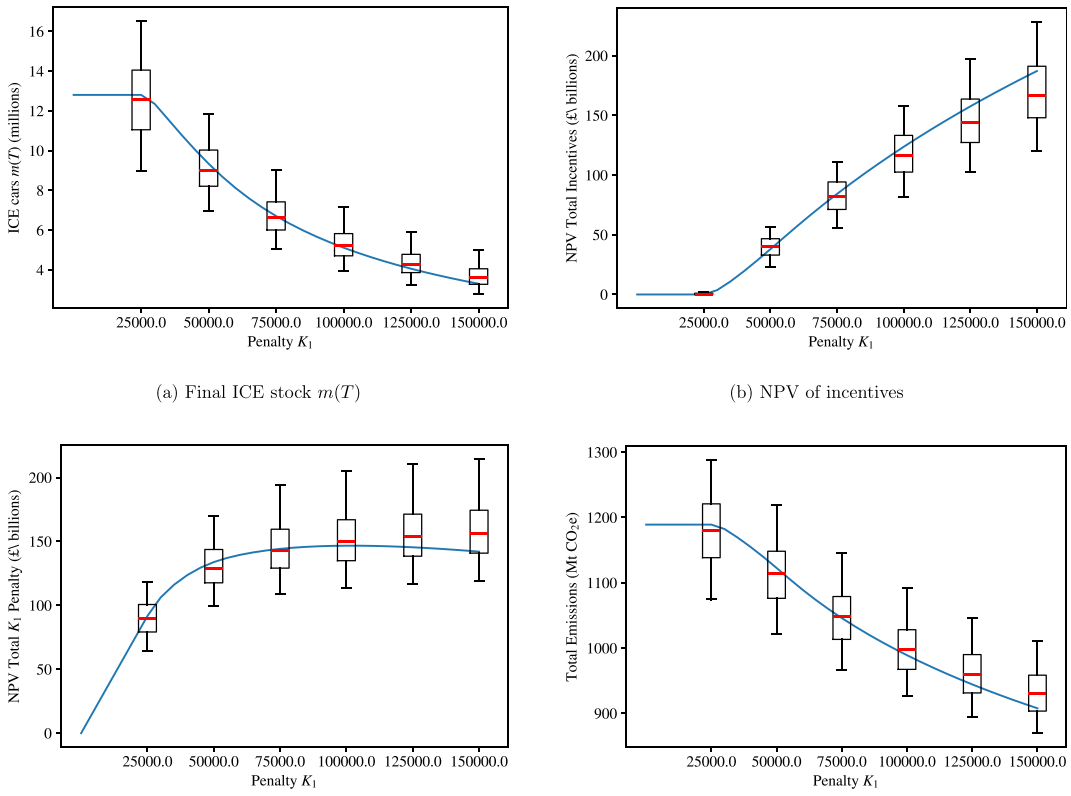
(a) Deterministic (b) Stochastic

Fig. 3. Optimal incentive paths and fleet dynamics under a large sales penalty ($K_2 = 30{,}000$, $K_1 = K_3 = 0$). Panel (a) reports the deterministic solution. Panel (b) reports the stochastic solution.

Early intervention becomes optimal because reducing ICE sales today avoids repeated flow penalties in all subsequent periods. Stated directly, the mechanism of a sales-flow penalty is that it prices every ICE transaction at the moment it occurs; each year of delayed intervention adds a further year of penalized sales, which is why optimal incentives are front-loaded.

Under this regime, stochastic incentives vary little across simulation paths. Uncertainty instead manifests in dispersion of the final ICE stock. Flow-based penalties therefore generate front-loaded but less adaptive policies compared to terminal penalties.

Overall, these results highlight a structural distinction between stock-based and flow-based policy instruments. Terminal penalties induce delayed but adaptive strategies that stabilize long-run fleet outcomes, whereas sales penalties generate immediate intervention with stronger early emission reductions but greater uncertainty in terminal stock composition.



(a) Final ICE stock $m(T)$

(b) NPV of incentives

(c) NPV of terminal penalties

(d) Cumulative emissions

Fig. 4. Effect of increasing the terminal penalty K_1 on policy outcomes. Panels report (a) the number of ICE vehicles in 2050, (b) the NPV of total incentive spending, (c) the NPV of terminal penalties, and (d) cumulative emissions. Other penalties are set to zero ($K_2 = K_3 = 0$).

5.2. Effect of penalties on outcomes

We next evaluate how alternative policy instruments affect long-run fleet composition, fiscal costs, and cumulative emissions. Outcome measures are defined formally in Appendix F. In particular, we report (i) the final ICE stock $m(T)$, (ii) the net present value (NPV) of incentive expenditures, (iii) the NPV of policy penalties, (iv) the NPV of fuel-tax revenues, and (v) cumulative CO_2e emissions over the period 2025–2050.

5.2.1. Terminal stock penalties

Fig. 4 illustrates how increasing the terminal penalty parameter K_1 in Eq. (8) affects optimal policy and fleet outcomes. Higher values of K_1 increase the shadow cost of remaining ICE vehicles at the horizon T, inducing stronger policy intervention.

As K_1 rises, the final ICE stock $m(T)$ declines monotonically, while the NPV of incentive expenditures increases. Cumulative emissions also fall, though more gradually than the terminal stock. This difference reflects structural fleet inertia in Eq. (5): changes in new sales translate only gradually into changes in the stock of vehicles on the road.

Quantitatively, large terminal penalties can reduce the ICE fleet in 2050 by two thirds relative to the no-intervention benchmark. However, achieving such reductions requires substantial fiscal outlays. On the computational grid used here, the implied intervention threshold lies between $K_1 = £25{,}000$ and £30,000: no intervention is optimal at the former value, whereas positive incentive provision emerges at the latter. Discounted to 2025, this corresponds to a substantially smaller present value, consistent with the intertemporal structure of Eq. (8).

5.2.2. Sales-based penalties

Fig. 5 reports outcomes when ICE sales are penalized continuously through the term $(1-\lambda)\nu_s K_2$ in Eq. (8). Unlike terminal penalties, sales penalties induce immediate intervention, because each additional ICE vehicle sold generates an instantaneous fiscal cost.

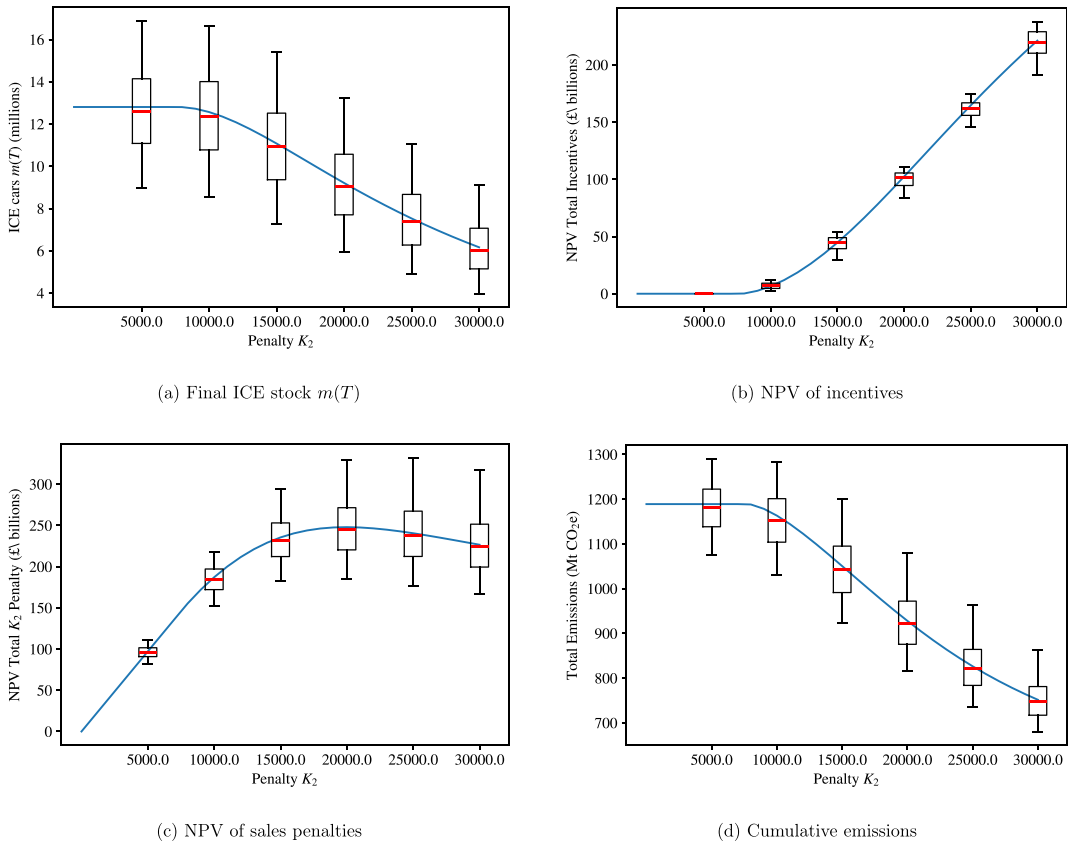
As K_2 increases, incentive spending rises and cumulative emissions decline. However, for comparable fiscal expenditure, sales penalties are less effective in reducing the final ICE stock $m(T)$ than terminal penalties. The reason is timing: flow-based penalties encourage early turnover, which lowers cumulative emissions, but they do not directly target the terminal stock.

On the computational grid used here, the intervention threshold under sales penalties lies in the range $K_2 \approx £7000$–£8000, numerically close to the discounted magnitude of the terminal-penalty threshold. This numerical proximity is consistent with the trade-off between immediate and delayed policy action embedded in the government's objective, although the two penalties apply to different objects and are not economically equivalent.

Overall, terminal penalties are more effective in shaping long-run fleet composition, whereas sales penalties deliver stronger reductions in cumulative emissions by accelerating early transition dynamics.

5.2.3. Policy guidance from the intervention thresholds

The two thresholds identified above can be read as calibration-conditional threshold ranges for the UK case. For the stock-based instrument, active incentive provision becomes part of the optimal policy once the government's valuation of the 2050 target lies in the range $K_1 \approx £25{,}000$–£30,000 per ICE vehicle remaining at the horizon; for the



(a) Final ICE stock $m(T)$

(b) NPV of incentives

(c) NPV of sales penalties

(d) Cumulative emissions

Fig. 5. Effect of increasing the sales penalty K_2 on policy outcomes. Panels report (a) the number of ICE vehicles in 2050, (b) the NPV of total incentive spending, (c) the NPV of sales penalties, and (d) cumulative emissions. Other penalties are set to zero ($K_1 = K_3 = 0$).

sales-based instrument, once the penalty attached to current ICE sales lies in the range $K_2 \approx$ £7000–£8000 per vehicle sold (both ranges reflect the resolution of the computational grids). These ranges apply to the main calibration, with the estimated charging coefficient $\beta_3 = 0.538$ and continued projected charging-infrastructure growth; as shown in Appendix A, setting $\beta_3 = 0$ preserves the delayed-versus-front-loaded timing comparison in the tested deterministic examples but materially changes the baseline and shifts the intervention thresholds downward; the fiscal-lock-in evidence in Section 5.2.4 concerns the main calibration. The two penalties apply to different objects: a one-off charge on the terminal stock, and a recurring charge on every ICE sale. Therefore they are not economically equivalent, although the discounted magnitude of the K_1 range ($K_1 e^{-r(T-t_0)} \approx$ £7200–£8600 at $r = 0.05$) is numerically close to the K_2 range. Below these valuations, the model prescribes minimal incentive spending; above them, optimal incentive budgets scale with the penalty level as shown in Figs. 4 and 5. We emphasize that K_1 and K_2 should be considered as calibrated shadow penalties, i.e., the implicit valuations of missing a fleet target or of marginal ICE sales, and not tax rates that could be implemented directly. Within the model, these penalties link the government's priorities to two concrete policy decisions: when to offer EV purchase incentives and how large those incentives should be.

5.2.4. *Fuel taxation and fiscal lock-in*

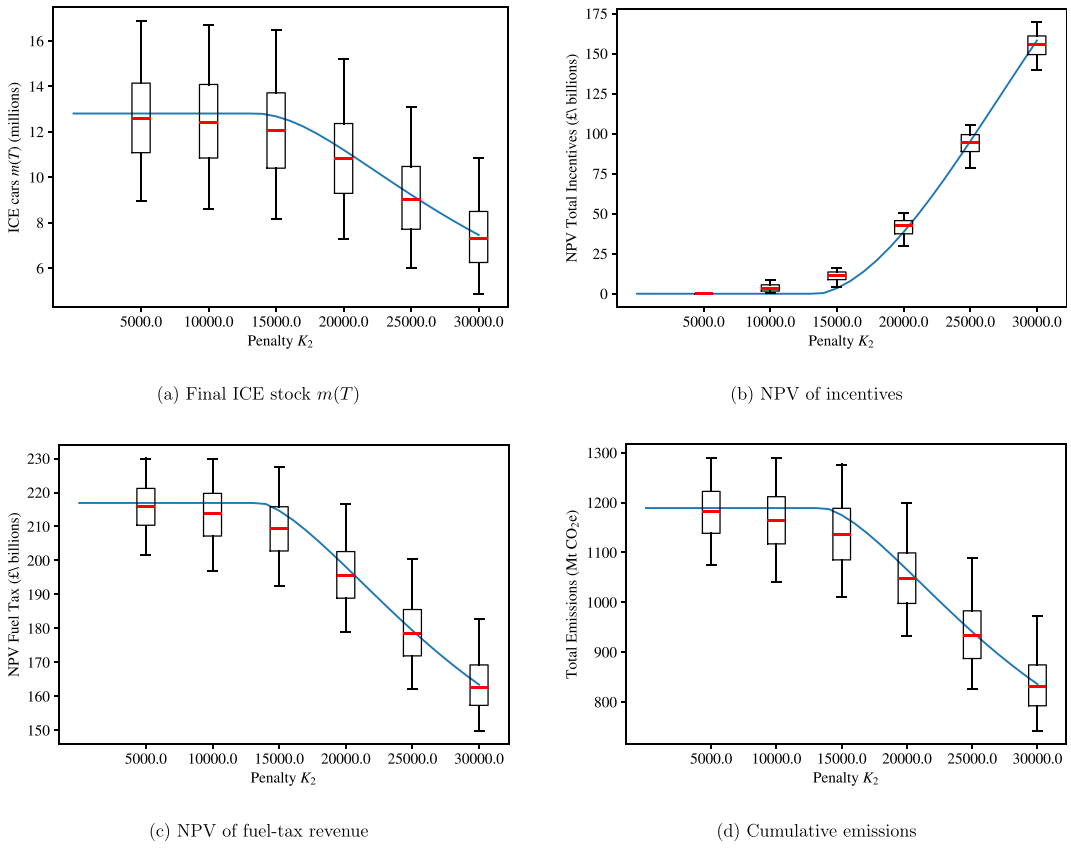
In practice, governments face a structural trade-off between environmental objectives and fiscal revenues. ICE vehicles generate substantial public income through fuel duties and carbon-related taxation. In the model, this channel enters the government objective through the term mK_3 in Eq. (8), where $K_3 < 0$ represents per-vehicle fuel-tax revenue. We see that introducing fuel-tax revenues modifies the optimal policy threshold. Electrification now implies a loss of future fiscal income, increasing the opportunity cost of reducing the ICE stock.

Fig. 6 illustrates the interaction between fuel taxation and sales penalties. Relative to the case without fuel revenues, optimal incentive levels are systematically lower for any given value of K_2. The government internalizes the foregone fuel-tax stream associated with a shrinking ICE fleet, which weakens the incentive to accelerate electrification.

Quantitatively, the present value of fuel-tax revenue per ICE vehicle is economically large. Given an average vehicle lifetime of approximately 16 years and discounting at rate r, the implied discounted value is of the same order of magnitude as the intervention threshold identified in Section 5.2. As a result, policy intervention becomes optimal only when the sales penalty exceeds both the decarbonization trigger and the implicit fiscal value of maintaining ICE vehicles.

This mechanism generates a form of fiscal lock-in. Even when terminal or sales penalties would otherwise justify aggressive electrification, fuel-tax dependence raises the marginal cost of reducing the ICE stock. In the absence of alternative revenue instruments, optimal policy may therefore delay or scale back intervention.

This result shows that fuel-tax dependence can materially affect the timing and strength of optimal electrification incentives, providing a strong rationale for considering transport decarbonization alongside broader tax reform. Replacing fuel-duty revenues with distance-based road pricing, congestion charges, or carbon-based vehicle taxation would reduce the fiscal distortion identified above and lower the intervention threshold. Such revenue-neutral transition mechanisms are consistent with the environmental tax reform literature, which emphasizes the joint design of climate policy and public finance.



(a) Final ICE stock $m(T)$

(b) NPV of incentives

(c) NPV of fuel-tax revenue

(d) Cumulative emissions

Fig. 6. Effect of including fuel-tax revenues ($K_3 = -556.21$) in the sales-penalty regime. Panels report (a) the number of ICE vehicles in 2050, (b) the NPV of total incentive spending, (c) the NPV of fuel-tax revenues, and (d) cumulative emissions. Terminal penalties are set to zero ($K_1 = 0$).

Overall, incorporating K_3 highlights that the timing and strength of optimal incentives for EVs depend not only on environmental targets but also on the structure of existing fiscal systems. A further fiscal channel that we do not model is origin-based vehicle taxation. Tariffs and import duties differentiated by vehicle origin would simultaneously alter relative vehicle prices and government revenues, and could therefore change both the demand side and the fiscal side of the framework. Incorporating such instruments might become especially important given the EU–China trade tensions and is a natural direction for future work. We do however return to the broader industrial and trade dimensions later in Section 5.5.

5.2.5. *Demand elasticity and policy effectiveness*

The effectiveness of fiscal incentives depends critically on consumer responsiveness. In the EV adoption Eq. (6), this responsiveness is governed by the parameter β_2, which measures the elasticity of EV demand with respect to the net-of-subsidy purchase price. In this sensitivity exercise, β_2 is varied after the baseline country calibration, holding the adoption intercept adjustment and exogenous price paths fixed. These scenarios therefore need not reproduce the original observed adoption share at the reference-year incentive.

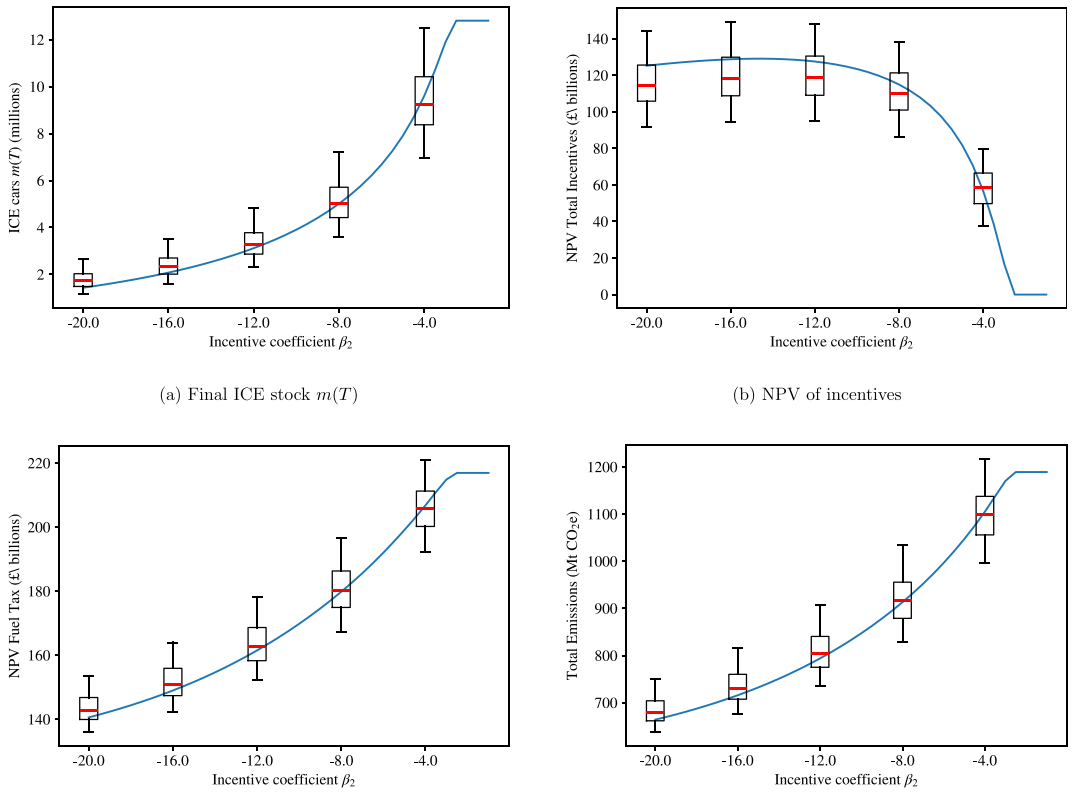
A larger absolute value of β_2 implies that a given subsidy induces a stronger increase in EV sales share $\lambda(t)$. Because incentive expenditures enter the objective function directly through the term $\lambda v_s \pi$ in Eq. (8), higher responsiveness increases the policy return per unit of fiscal spending.

Fig. 7 shows how varying β_2 affects long-run outcomes. When the absolute value of β_2 is small, EV adoption responds weakly to subsidies. In this case, even substantial fiscal effort produces only limited reductions in the ICE stock, and optimal policy converges toward relatively modest incentive provision.

As $|\beta_2|$ increases, incentives become more cost-effective. For a given penalty structure, higher responsiveness lowers the final ICE stock, reduces cumulative emissions, and decreases reliance on fuel-tax revenues. Importantly, the NPV of incentive spending does not necessarily increase monotonically with $|\beta_2|$. Because each unit of subsidy generates a larger behavioral response, the government can achieve environmental targets with lower fiscal outlays.

This result highlights that policy effectiveness depends not only on the scale of spending, but also on institutional and market conditions that shape demand responsiveness. We stress that β_2 is a calibrated constant in our framework, so we do not estimate how complementary measures, such as charging infrastructure expansion, information provision, regulatory simplification, or stable long-term policy signals, may change the effective elasticity of adoption. The sensitivity analysis should instead be read as quantifying how much such responsiveness would be worth if it could be achieved: in environments with higher $|\beta_2|$, incentive-based strategies deliver both stronger emission reductions and improved fiscal efficiency, so measuring and fostering demand responsiveness is itself a policy-relevant objective.

Overall, the parameter β_2 emerges as a pivotal determinant of optimal policy design. Where responsiveness is low, large-scale subsidies are rarely cost-effective. Where responsiveness is high, well-timed incentives can substantially accelerate the transition while limiting fiscal exposure.



(a) Final ICE stock $m(T)$

(b) NPV of incentives

(c) NPV of fuel-tax revenues

(d) Cumulative emissions

Fig. 7. Effect of varying the incentive elasticity parameter β_2 under combined terminal and sales penalties ($K_1 = 50{,}000$, $K_2 = 15{,}000$, $K_3 = -556.21$). Panels report (a) the number of ICE vehicles in 2050, (b) the NPV of total incentive spending, (c) the NPV of fuel-tax revenues, and (d) cumulative emissions.

5.3. Emissions timing: Early versus delayed intervention

The instruments compared above differ not only in cumulative emissions but in *when* emission reductions occur. To make this explicit, we compute annual emission paths $\eta\, m(t)$ and cumulative emissions over 2025–2030, 2025–2040, and 2025–2050, for the no-intervention baseline, and for the two example regimes in Section 5.1. All three trajectories are evaluated on the same uniform solver grid with the same converged smoothing parameters, and cumulative values use the quadrature in Appendix F. All values are physical tonnes of CO_2e, reported undiscounted.

Table 6 and Fig. 8 show that the sales-flow regime, which intervenes immediately, achieves a substantial share of its emission savings early: relative to the baseline it saves roughly 28 Mt by 2030 and 237 Mt by 2040, out of 437 Mt by 2050. The terminal-stock regime, by contrast, remains close to the baseline through 2030, with intervention beginning only near the end of the decade, and diverges more strongly as incentives ramp up toward the horizon; of its 199 Mt total savings by 2050, roughly three quarters accrue after 2040. Earlier reductions are therefore particularly relevant when policymakers place weight on interim carbon budgets or on the temporal profile of cumulative emissions. For a policymaker who attaches importance to the temporal profile of abatement,

Table 6
Cumulative CO_2e emissions from the UK ICE fleet under alternative deterministic policy regimes. Emissions are computed as $\eta\, m(t)$ with $\eta = 1.880$ tonnes per ICE vehicle per year on the uniform solver grid, accumulated to each horizon with the left-endpoint sum in Appendix F, and are not discounted.

Policy regime	Cumulative CO_2e emissions (Mt)		
	2025–2030	2025–2040	2025–2050
No intervention ($\pi = 0$)	299	838	1189
Terminal penalty ($K_1 = 100{,}000$)	299	789	990
Sales penalty ($K_2 = 30{,}000$)	271	601	752
Terminal & Fuel Tax ($K_1 = 100{,}000$ $K_3 = -556.21$)	299	811	1038
Sales & Fuel Tax ($K_2 = 30{,}000$ $K_3 = -556.21$)	277	648	836

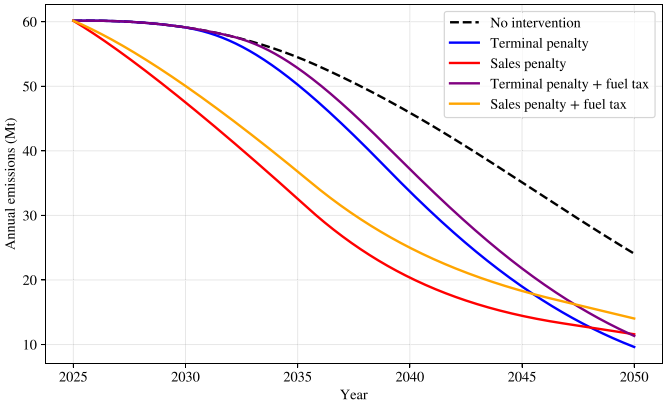


Fig. 8. Annual CO_2e emissions $\eta\, m(t)$ from the UK ICE fleet under no intervention (black dashed line), a terminal-stock penalty ($K_1 = 100{,}000$ blue line), and a sales-flow penalty ($K_2 = 30{,}000$ red line). The terminal and sales penalties are run a second time with fuel tax ($K_3 = -556.21$) included. (For interpretation of the references to colour in this figure legend, the reader is referred to the web version of this article.)

this timing asymmetry is a substantive argument for flow-based instruments or for combining them with stock-based targets, beyond the cost comparisons of the previous subsections.

Including fuel-tax revenue in the government objective weakens the emissions reductions achieved under both policy regimes. Under the terminal-stock penalty, cumulative emissions fall by 151 Mt relative to the no-intervention baseline by 2050 when fuel-tax revenue is included, compared with 199 Mt when it is excluded. Under the sales-flow penalty, the corresponding 2050 reduction falls from 437 Mt to 353 Mt. The timing effect differs across the two instruments. In the terminal regime, accounting for foregone fuel-tax revenue delays the onset of intervention and therefore further back-loads emissions reductions. By contrast, the sales-based regime continues to intervene from the start of the simulation, but at a lower intensity, so that its emissions advantage is reduced at each horizon while remaining strongly front-loaded. Thus, fuel-tax dependence does not overturn the distinction between the two policy objectives, but it weakens the pace of decarbonization generated by both. The policy implication is to plan for the budgetary consequences of declining fuel-tax revenues alongside EV incentive programs.

5.4. Cross-country robustness: France

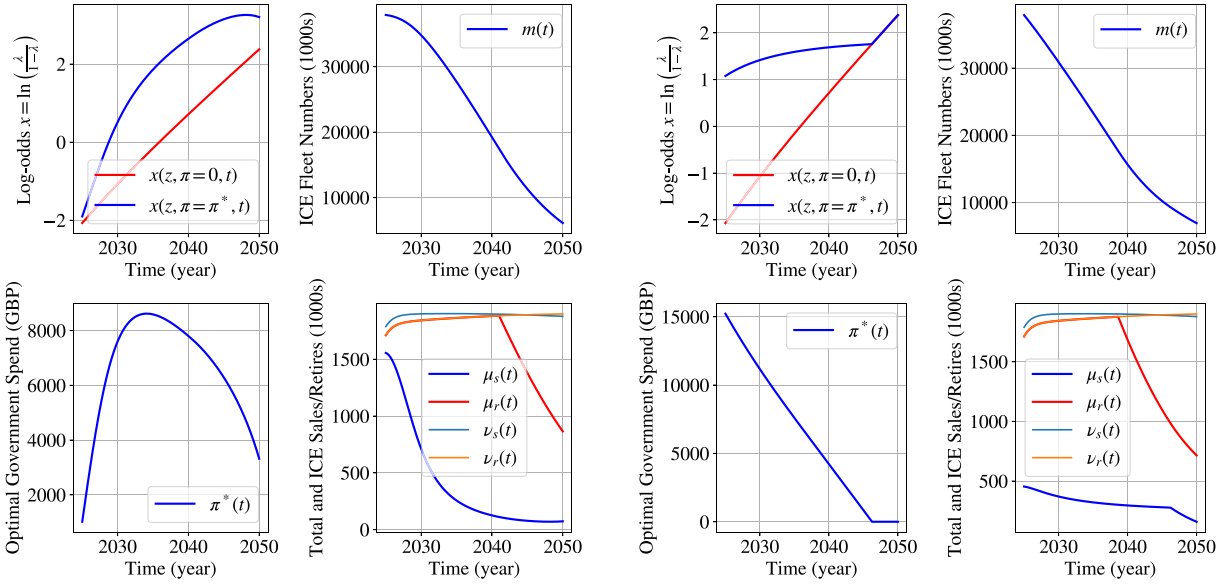
To assess whether the qualitative policy mechanisms identified in the UK calibration depend on the UK institutional setting, we repeat the deterministic analysis using a country-specific calibration for France. The same model structure and estimated adoption coefficients are retained, while fleet dynamics, population, observed vehicle prices and adoption, charging infrastructure, vehicle retirement, and fiscal parameters are recalibrated using French data. Country-specific calibration details for the UK and France are reported in Appendix D. We are therefore able to show how our framework could be applied in a different setting and what changes to the structure of the optimal policy might arise.

We can directly compare the earlier results for the UK, Figs. 2(a) and 3(a), to the strategies derived for France in Fig. 9(a) and (b) respectively. This shows that the broad distinction between terminal- and sales-based objectives carries over to the French calibration, but with important differences in timing relative to the UK case. Under the terminal-stock penalty, intervention begins immediately rather than after an initial period of inactivity (see Fig. 2a). The optimal incentive rises to a maximum of just over £8000 per vehicle around the mid-2030s before declining toward the end of the horizon. The adjustment of the ICE fleet is comparatively gradual, reflecting the older French vehicle stock and the higher calibrated retirement ages. Under the sales penalty, incentives also begin immediately but decline more steadily over time, approaching zero before 2050. The resulting policy path is qualitatively similar to the UK sales-based case.

The French application therefore qualifies the timing result obtained from the UK calibration. In particular, a terminal-stock objective does not necessarily imply an initial period of zero intervention: whether such a delay is optimal depends on country-specific fleet composition, turnover dynamics, and demand conditions. One possible explanation is that the French car fleet has a slower turnover than that of the UK, with model implied average age at retirement T_∞ closer to 21 in France compared to 16 in the UK. At the same time, the similarity of the sales-based policy paths across the two countries partly reflects the common prospective assumptions governing vehicle-price trends and charging-infrastructure growth. The comparison therefore supports the portability of the modeling framework while showing that the timing and intensity of the optimal policy remain sensitive to country-specific calibration and to assumptions about the evolution of the broader EV market.

5.5. Scope of the framework: Manufacturing, employment, and trade

Our model focuses on the government's fiscal problem. It treats vehicle supply, prices, and production location as exogenous and examines how governments should time purchase incentives given fleet inertia and feedback. The wider literature also highlights the industrial dimension of vehicle electrification, showing how manufacturing capabilities, employment, supply chains, trade balances, and industrial policy shape governments' incentives to accelerate or resist the transition. For



(a) Terminal Penalty

(b) Sales Penalty

Fig. 9. Optimal incentive paths and fleet dynamics for the French calibration, under (a) a large terminal penalty ($K_1 = 100{,}000$, $K_2 = K_3 = 0$) or (b) sales penalty ($K_1 = 0$, $K_2 = 30{,}000$, $K_3 = 0$). Both report the deterministic solution obtained via Pontryagin's Minimum Principle. All monetary inputs and outputs are converted to GBP for easier comparison with UK.

example, Altenburg et al. (2022) document how China's electromobility push combined environmental goals with a deliberate catch-up and competitive-advantage strategy; Meckling and Nahm (2019) show that technology-ban announcements for ICE vehicles are driven as much by industrial-policy competition as by climate goals; and Rísquez Ramos and Ruiz-Gálvez (2024) trace how electrification reorganizes automotive value chains, with substantial consequences for inter-plant competition, employment, and supplier networks.

These channels are not irrelevant to our setting – for a country with a large domestic automotive sector, they may be first-order. Within our framework they would enter in two ways. First, an extended welfare objective could add terms for domestic value added, employment, or the trade balance, so that the effective penalties on ICE sales and stocks would no longer reflect climate targets alone: a government protecting a domestic ICE supply chain would behave as if K_1 and K_2 were lower, delaying intervention, while a government seeking first-mover advantage in EV manufacturing would behave as if they were higher. Second, the interpretation of the calibrated penalties changes: our K_1 and K_2 thresholds should be read as *net* valuations that, in practice, already embody whatever weight a government places on industrial consequences. Endogenizing manufacturing location, employment, or trade flows would require firm- and plant-level data and a supply-side model that are beyond the scope of this paper, and we therefore do not attempt it here; the UK case, where domestic vehicle production is modest relative to the fleet, limits but does not eliminate the resulting bias. Extending the framework in this direction, including origin-based vehicle taxation and tariff instruments (Section 5.2.4), is a promising avenue for future research.

6. Conclusions

This paper develops a dynamic policy evaluation framework to study how governments can design and time fiscal incentives to accelerate the transition from internal combustion engine (ICE) vehicles to electric vehicles (EVs). By integrating empirically calibrated adoption behavior with long-horizon fleet dynamics and uncertainty in EV costs, the model provides a transparent structure for comparing alternative policy regimes on consistent fiscal and environmental grounds. As a result, three main policy insights emerge.

First, the timing of intervention fundamentally shapes long-run outcomes. Policies that penalize the remaining ICE stock at a terminal date tend to generate more back-loaded and adaptive incentive paths, although the onset of intervention depends on country-specific calibration. By contrast, sales-based penalties generate more strongly front-loaded intervention, reducing cumulative emissions earlier but exerting weaker control over final fleet composition. This distinction highlights that instruments targeting stock outcomes (such as phase-out mandates or binding long-run targets) and instruments targeting sales flows (such as feebates or emissions standards) are not interchangeable: they imply structurally different transition paths.

Second, the analysis reveals a fiscal lock-in mechanism. As long as ICE vehicles generate substantial fuel-tax revenues, electrification entails a direct loss of public income. When these revenues are internalized in the government objective, optimal incentives are systematically weaker, while the effect on intervention timing depends on the policy objective. Without credible replacement mechanisms for declining fuel-duty revenues, such as distance-based road pricing or broader carbon taxation, governments may face stronger fiscal incentives to slow the pace of electrification even under binding climate targets.

Third, consumer responsiveness to incentives is pivotal. When demand reacts weakly to subsidies, large-scale fiscal programs deliver limited emission reductions relative to their cost. Conversely, higher responsiveness substantially improves policy efficiency, lowering both cumulative emissions and required fiscal outlays. This underscores that the effectiveness of a given subsidy depends critically on the degree of consumer responsiveness. Identifying which complementary policies causally increase that responsiveness remains an important question for future research.

Taken together, the results reinforce the importance of coherent and forward-looking climate policy. Delayed intervention increases the risk of abrupt and fiscally costly adjustments near policy deadlines, while fragmented instruments may fail to align short-run incentives with long-run fleet objectives. By explicitly linking sales dynamics, stock evolution, fiscal revenues, and uncertainty, the framework clarifies how alternative policy objectives translate into distinct incentive paths over multi-decade horizons.

Two caveats bound the scope of these conclusions. First, while the modeling framework is applied to both the UK and France, the quantitative findings we show including intervention thresholds and fiscal magnitudes remain country-specific and should not be extrapolated without recalibrating fleet dynamics, prices, incentives, and fiscal parameters. The French application provides evidence on the robustness of the qualitative mechanisms across two national settings, although there are many underlying similarities between the two. Second, the analysis abstracts from distributional effects, heterogeneous households, and the supply side of the vehicle market: manufacturing, employment, supply chains, trade balances, and industrial-policy competition are not modeled, even though they can materially shape a government's effective valuation of the transition, and origin-based vehicle taxation and tariffs may alter the fiscal structure we take as given. Future research could extend the framework to incorporate income heterogeneity, regional infrastructure deployment, endogenous technological learning, and these industrial and trade channels. Nonetheless, the present model demonstrates that effective transport decarbonization requires more than sustained subsidy levels. The results therefore support coordinated policy design that aligns long-run targets, short-run incentives, and fiscal sustainability, while recognizing that the appropriate combination of instruments will depend on country-specific institutional and market conditions.

CRediT authorship contribution statement

Paul Vincent Johnson: Writing – original draft, Visualization, Software, Methodology, Investigation, Conceptualization. **Dávid Zoltán Szabó:** Writing – review & editing, Validation, Methodology, Formal analysis, Conceptualization.

Declaration of Generative AI and AI-assisted technologies in the writing process

During the preparation of this work, the authors used ChatGPT (OpenAI) and Claude (Anthropic) to assist with language editing, manuscript revision, code development, numerical analysis, and reproducibility checks. The authors reviewed and edited the outputs as needed and take full responsibility for the content of the published article.

Declaration of competing interest

The authors declare that they have no known competing financial interests or personal relationships that could have appeared to influence the work reported in this paper.

Appendix A. Empirical robustness checks

This appendix reports robustness checks for the EV adoption equation estimated in Section 4. Given the short time dimension (2021–2024) and the aggregate country-level data, we wish to verify that the main elasticity results are not driven by distributional assumptions. To relax the beta-distribution assumption, we re-estimate the EV sales share equation using a fractional logit model following Papke and Wooldridge (1996). The dependent variable remains the EV sales share $\lambda_{it} \in (0, 1)$.

Table A.7
Fractional logit robustness estimates using country-clustered standard errors.

	Fractional Logit (Country & Year FE)
$\ln(P_{EV}/P_{ICE})$	−2.317***
	(0.444)
$\ln(1-\pi/P_{EV})$	−4.315**
	(1.698)
$\ln(C_p)$	0.033
	(0.210)
Country FE	Yes
Year FE	Yes
Clustered SE	Yes (Country)
Observations	56
Pseudo R^2 (CS)	0.283

Estimation is implemented as a binomial generalized linear model with logit link (quasi-maximum likelihood), and the results are reported in Table A.7. We include country and year fixed effects and compute standard errors clustered at the country level.

The relative price elasticity remains negative and statistically significant under the fractional logit specification, and its magnitude is consistent with the beta regression estimates reported in Table 5. The incentive coefficient retains its negative sign and remains significant at the 5% level, though it is less precisely estimated than in the beta regressions, reflecting limited within-country time variation.

The charging infrastructure coefficient becomes small and statistically insignificant once country fixed effects are introduced, suggesting that part of the cross-country correlation reflects structural differences rather than short-run causal effects.

To examine sensitivity to the charging contribution, we consider an alternative calibration with $\beta_3 = 0$. The country adoption adjustment δ_{UK} is recomputed using Eq. (9), while observed vehicle prices and incentives, the exogenous price projections, and the remaining demand coefficients are held fixed. Both calibrations therefore reproduce the same observed adoption share at the reference-year incentive, without changing vehicle prices to obtain that match. In the tested deterministic examples ($K_1 = 100{,}000$; $K_2 = 30{,}000$; the threshold neighborhoods; all with $K_3 = 0$), the delayed-versus-front-loaded timing comparison is preserved, but the quantitative baseline is materially affected: without the projected infrastructure-driven adoption drift, the no-intervention ICE stock in 2050 rises from 12.8 to 28.4 million. Intervention nevertheless becomes optimal at lower terminal-penalty levels than in the main calibration; for example, at $K_1 = 25{,}000$ the optimal policy begins around 2036, reaches a maximum incentive of about £9300, and has an incentive NPV of approximately £48.2 billion. Because these checks set $K_3 = 0$, they do not speak to the fuel-tax channel; the fiscal-lock-in evidence of Section 5.2.4 concerns the main calibration. The two example policies also have different incentive budgets, and their ranking by terminal ICE stock differs between the two calibrations, so these comparisons do not establish general superiority of either instrument at equal cost. The baseline projections in the main text should therefore be read as conditional on continued charging-infrastructure expansion at the calibrated rate, together with the cross-sectional association captured by β_3.

To summarize, the timing contrast between stock-based and sales-based penalties is robust in the tested examples, whereas the quantitative fleet projections, spending levels, and intervention thresholds are calibration-sensitive. This is particularly true for the charging-infrastructure channel.

Appendix B. Construction of the cross-country EV policy dataset

This appendix documents the construction of the cross-country dataset used to estimate EV adoption and calibrate the policy model. The objective is to obtain harmonized, sales-weighted measures of (i) vehicle prices, (ii) EV purchase incentives, and (iii) EV market shares across countries for the period 2021–2024.

All monetary values are converted to USD using annual average exchange rates. Incentives are expressed as sales-weighted averages per EV sold in each country-year.

B.1. Data sources

The dataset combines the following sources:

- National vehicle registration statistics (market shares and sales volumes)
- International Energy Agency (IEA) price and adoption statistics
- Government publications on purchase grants and tax rules
- National tax authority documentation
- Industry price databases for MSRP reconstruction (where official sales-weighted prices are unavailable)

Where official sales-weighted prices were unavailable, we reconstruct average MSRPs using top-selling model lists and apply reported discounts when available.

B.2. Definition of incentives

For each country c and year t, we define the average EV incentive as:

$$\bar{\pi}_{c,t} = \lambda_{BEV,c,t}\pi_{BEV,c,t} + \lambda_{PHEV,c,t}\pi_{PHEV,c,t}, \tag{B.1}$$

where $\lambda_{BEV,c,t}$ and $\lambda_{PHEV,c,t}$ are sales shares among EVs, and $\pi_{BEV,c,t}$ and $\pi_{PHEV,c,t}$ denote total fiscal support per vehicle.

Total fiscal support includes:

- Direct purchase grants
- Registration tax exemptions
- VAT exemptions or reductions
- Circulation/ownership tax exemptions (5-year NPV)
- Benefit-in-kind (BiK) tax advantages (3-year lease NPV)
- Import duty exemptions where applicable

Fuel tax advantages are excluded from $\bar{\pi}_{c,t}$ and instead enter the government objective through parameter K_3.

All multi-year tax benefits are converted into net present values using a 5% annual discount rate.

B.3. Price construction

Let $P_{EV,c,t}$ and $P_{ICE,c,t}$ denote sales-weighted MSRPs. When official averages are unavailable, prices are constructed as:

1. Identify top-selling models by drivetrain.
2. Obtain list prices for registration year t.
3. Apply reported average transaction discounts when available.
4. Compute sales-weighted averages.

In countries lacking detailed data (e.g., Spain, Netherlands, Italy), we benchmark EV–ICE price differentials against comparable EU markets with similar segment composition.

B.4. Treatment of corporate tax benefits

Where company car taxation materially affects EV adoption (e.g., UK, Germany, Sweden, and the Netherlands), we compute the fiscal value of Benefit-in-Kind (BiK) reductions as:

$$\text{BiK Saving} = \Delta\tau \cdot \tau_{inc} \cdot s_{corp} \sum_{i=0}^{L-1} (1+r)^{-i} \cdot P_{EV,c,t}, \tag{B.2}$$

where $\Delta\tau$ is the tax rate differential between ICE and EV vehicles, τ_{inc} is the marginal income tax rate, s_{corp} is the share of company cars, L is the lease length, and r is the discount rate.

B.5. Harmonization across jurisdictions

Given substantial heterogeneity in tax systems, three harmonization rules are applied:

1. All incentives are expressed in per-vehicle USD equivalents.
2. Temporary mid-year policy changes are annualized using sales timing where available.
3. Caps on VAT or registration exemptions are applied to the reconstructed MSRP.

B.6. Measurement limitations

Three limitations should be noted. First, in several countries (e.g., Spain, Italy, Netherlands), sales-weighted prices are not officially published and must be reconstructed from model-level data. Second, eligibility constraints (income caps, domestic content rules) are incorporated using observed qualification rates when available, and approximated otherwise. Third, some regional or local incentives apply only to subsets of buyers. In these cases, incentives are weighted by estimated eligibility shares. These approximations introduce measurement noise but do not affect the structural interpretation of the model, which relies primarily on cross-country variation and time-series policy changes.

B.7. Country-specific implementation

Detailed country-by-country constructions underlying $\bar{\pi}_{c,t}$ are summarized in Table 3, with the corresponding EV sales shares, vehicle prices, and charging infrastructure reported in Tables 1 and 2, and 4.

All values used in the estimation of the EV adoption function in Section 4 are directly constructed from these tables.

Appendix C. Fleet turnover and retirement structure

This appendix provides the explicit functional forms underlying the fleet turnover and retirement structure described in Sections 3.1 and 3.2. The purpose is to ensure full transparency and reproducibility of the dynamic model.

A. Total fleet turnover

Let $n(t)$ denote total fleet size and $T_r(t)$ the average retirement age. We approximate the age distribution of vehicles using a linear density over the interval $[0, T_r(t)]$. Specifically, let the density of vehicles of age τ at time t be

$$f(\tau, t) = \nu_s(t) + \alpha(t)\tau, \qquad 0 \le \tau \le T_r(t), \tag{C.1}$$

where $\nu_s(t)$ represents the inflow of new vehicles and $\alpha(t)$ captures the slope of the age distribution.

Total fleet size satisfies

$$n(t) = \int_0^{T_r(t)} f(\tau, t)\, d\tau = \nu_s(t) T_r(t) + \frac{1}{2}\alpha(t) T_r^2(t). \tag{C.2}$$

Differentiating (C.2) with respect to time yields a relationship between fleet growth, retirement age dynamics, and the slope parameter $\alpha(t)$. Solving for total sales gives

$$\nu_s(t) = \frac{n(t)}{T_r(t)} - \frac{1}{2}\alpha(t) T_r(t). \tag{C.3}$$

Total retirements are defined as

$$\nu_r(t) = \nu_s(t) - \frac{dn(t)}{dt}, \tag{C.4}$$

which is consistent with the fleet balance Eq. (2). This formulation ensures internal consistency between sales, retirements, fleet size, and retirement age dynamics.

B. ICE-specific retirement allocation

Let $m(t)$ denote the stock of ICE vehicles and $s_m(t)$ their cumulative age. The average age of the ICE fleet is therefore $s_m(t)/m(t)$.

The evolution of cumulative ICE age satisfies

$$\frac{ds_m}{dt} = m(t) - \Psi(t)\,\mu_r(t), \tag{C.5}$$

where

$$\Psi(t) = \max\left(T_r(t), \frac{s_m(t)}{m(t)}\right) \tag{C.6}$$

represents the effective retirement age applied to the ICE fleet.

Total retirements $\nu_r(t)$ must be allocated between ICE and EV vehicles. We model ICE retirements as proportional to total retirements, weighted by the relative age structure of the ICE fleet compared to the total fleet.

Define $s_n(t)$ as total cumulative fleet age. The ICE retirement flow is given by

$$\mu_r(t) = \omega(t)\,\nu_r(t), \tag{C.7}$$

where the weight $\omega(t)$ satisfies

$$\omega(t) = \max\left(0, \min\left(\frac{3s_m(t) - m(t)T_r(t)}{3s_n(t) - n(t)T_r(t)}, 1\right)\right). \tag{C.8}$$

This functional form has three desirable properties:

1. $0 \le \mu_r(t) \le \nu_r(t)$ (retirements are bounded),
2. older ICE fleets retire faster relative to the total fleet,
3. the rule remains stable even when fleet composition changes rapidly.

Together, Eqs. (C.3)–(C.7) fully determine the turnover structure used in the numerical simulations.

Appendix D. Country specific calibrations

The initial age-state variables are constructed consistently with the calibrated aggregate age stock. For the UK calibration, $s_n(t_0) = 271.665$ million car-years and $s_m(t_0) = 267.392$ million car-years, implying model-state mean ages $a_n(t_0) = 7.998$, $a_p(t_0) = 2.165$, and $a_m(t_0) = 8.358$ years. For the French calibration, $s_n(t_0) = 428.725$ million car-years and $s_m(t_0) = 424.136$ million car-years, implying model-state mean ages $a_n(t_0) = 10.789$, $a_p(t_0) = 2.490$, and $a_m(t_0) = 11.192$ years. French fleet-stock and age data are taken from SDES (Service des données et études statistiques (SDES), 2025), while the population path is based on the INSEE central population projection (INSEE, 2021). French fuel-tax parameters are constructed from national excise rates and driving-distance data (Légifrance, 2024; Service des données et études statistiques (SDES), 2025); vehicle prices, incentives, adoption, and charging density use the harmonized sources described in Section 4.

Tables D.8 and D.9 summarize the calibration used in the UK and France applications. Table D.8 reports the country-specific initial conditions, projected population and fleet levels, retirement-function parameters, and fuel-tax calibration. Table D.9 collects the parameters held fixed across the two applications, including the pooled demand coefficients and the common assumptions governing price trends, charging-infrastructure growth, and EV-price dynamics. This separation makes it clear which differences in the simulated outcomes arise from country-specific calibration and which reflect structural assumptions shared across both applications.

Table D.8
Country-specific calibration parameters, initial conditions, and projected population and fleet size for the United Kingdom and France.

Parameter/initial condition	UK	France
Simulation start t_0	2025	2025
Demand anchor year t_a	2024	2024
Population $P(t_0)$ (million)	69.799	68.011
Total fleet n_0 (million)	33.967	39.739
Plug-in stock p_0 (million)	1.974	1.843
ICE/non-plug-in stock m_0 (million)	31.993	37.896
Initial plug-in share (%)	5.812	4.638
Country adoption adjustment δ_c	0.0662	−0.0354
Population $P(2050)$ (million)	76.919	69.196
Total fleet $n(2050)$ (million)	37.432	40.432
T_0	13.190	19.880
T_∞	16.018	21.404
γ_r	0.723	1.027
t_r	2022.109	2022.680
K_3 (£ per ICE vehicle-year)	−556.21	−517.51

Table D.9
Common model and projection parameters used in the UK and France applications. The demand coefficients are estimated from the pooled cross-country sample; country-specific adoption adjustments are reported separately.

Parameter	Symbol	Value
Discount rate	r	0.05
Terminal year	T	2050
Pooled demand intercept	β_0	−5.509
Relative-price coefficient	β_1	−2.056
Incentive coefficient	β_2	−6.457
Charging-infrastructure coefficient	β_3	0.538
EV price trend	θ_1	−0.005
ICE price trend	θ_2	0.020
Charging-infrastructure growth rate	θ_3	0.200
Initial EV-price deviation	z_0	0.250
Mean-reversion rate	κ	0.100
ICE emissions factor	η	1.880 tonnes CO_2e/(vehicle-year)

Appendix E. Numerical solution methods

This appendix describes the numerical procedures used to solve the optimal control problem. These details are provided for completeness and reproducibility. All numerical settings are documented where required, and the analysis code is available from the authors on request. All demand evaluations, optimal-control calculations and forward simulations use the effective intercept $\beta_0 + \delta_c$. The adjustment is constant within each scenario; it changes the evaluated demand function but not the form of the optimality conditions.

E.1. Deterministic optimal control via pontryagin's minimum principle

In the limit $\sigma \to 0$, the stochastic control problem reduces to a deterministic optimal control problem. In this case, the state trajectory becomes non-random, and the system may be analyzed using Pontryagin's Minimum Principle (PMP). Specifically, since

$$z(t) = z(t_0)\, e^{-\kappa(t-t_0)},$$

the state variable z evolves deterministically, and thus the demand function can be expressed in the reduced form $\lambda(\pi, t)$.

The state dynamics are then given by

$$m'(t) = (1 - \lambda(\pi, t))v_s - \mu_r(m, s_m), \tag{E.1}$$

$$s_m'(t) = m - \Psi(m, s_m)\mu_r(m, s_m), \tag{E.2}$$

where $\mu_r(m, s_m)$ denotes the ICE retirement flow introduced in Section 3.2, and

$$\Psi(m, s_m) = \max\left(T_r, \frac{s_m}{m}\right).$$

The instantaneous cost rate is

$$L(m, s_m, \pi, t) = e^{-r(t-t_0)}\left[\lambda(\pi, t)v_s\pi + (1 - \lambda(\pi, t))v_s K_2 + mK_3\right].$$

Hamiltonian. Introducing costate variables $c_1(t), c_2(t)$ corresponding to m and s_m, the Hamiltonian is

$$H(m, s_m, c_1, c_2, \pi, t) = L(m, s_m, \pi, t) + m'c_1 + s_m'c_2, \tag{E.3}$$

and the optimal Hamiltonian is given by the following

$$\hat{H}(m, s_m, c_1, c_2, t) = \inf_{\pi \in [0, \pi_{\max}]} H(m, s_m, c_1, c_2, \pi, t).$$

Adjoint system. By PMP (see e.g., (Fleming and Soner, 2006, Eq. (6.2))), the costate dynamics satisfy

$$\frac{dc_1}{dt} = \frac{\partial \mu_r}{\partial m}c_1 - c_2 + \left(\frac{\partial \Psi}{\partial m}\mu_r + \Psi\frac{\partial \mu_r}{\partial m}\right)c_2 - K_3 e^{-r(t-t_0)}, \tag{E.4}$$

$$\frac{dc_2}{dt} = \frac{\partial \mu_r}{\partial s_m}c_1 + \left(\frac{\partial \Psi}{\partial s_m}\mu_r + \Psi\frac{\partial \mu_r}{\partial s_m}\right)c_2. \tag{E.5}$$

When future costs are discounted, the costates are linked to the value function V by

$$(c_1, c_2) = e^{-r(t-t_0)}\left(\frac{\partial V}{\partial m}, \frac{\partial V}{\partial s_m}\right).$$

Optimality condition. Since $\beta_2 < 0$ and $0 < \lambda(\pi, t) < 1$, the Hamiltonian is convex in π. The unique minimizer $\pi^*(t)$ satisfies the first-order condition

$$\frac{\partial H}{\partial \pi}(m, s_m, c_1, c_2, \pi, t) = 0, \tag{E.6}$$

which can be written explicitly as

$$1 + \frac{\pi - c_1 e^{r(t-t_0)} - K_2}{\pi - P_{\text{EV}}}\,\beta_2(1 - \lambda(\pi)) = 0. \tag{E.7}$$

Convexity ensures uniqueness of the solution; if the First Order Condition (FOC) in Eq. (E.7) yields $\pi < 0$, the admissible control saturates at $\pi = 0$.

Boundary value problem. The optimal trajectory is obtained by solving the coupled system (E.1), (E.2), (E.4), (E.5), subject to

$$m(t = t_0) = m_0, \qquad s_m(t = t_0) = s_0, \tag{E.8}$$

and

$$c_1(t = T) = K_1 e^{-r(T-t_0)}, \qquad c_2(t = T) = 0. \tag{E.9}$$

Because $c_1(t_0), c_2(t_0)$ are not known a priori, a shooting method is employed in which initial guesses are iteratively updated until the terminal conditions are satisfied.

Although μ_r and Ψ are piecewise differentiable, numerical solution requires smoothing these functions to ensure Lipschitz continuity and differentiability of the ODEs. The smoothing factor is then reduced gradually until convergence is achieved. Optimality of the resulting control is later verified by comparison with the dynamic programming solution in Section 5.

E.2. Stochastic optimal control – Dynamic programming

We consider the stochastic optimal control problem, where the associated Hamilton–Jacobi–Bellman (HJB) equation takes the form

$$\frac{DV}{Dt} + \mathcal{L}_z\{V\} + \lambda(z,\pi)v_s\pi + (1-\lambda(z,\pi))v_sK_2 + mK_3 = 0,$$

with

$$\frac{DV}{Dt} = \frac{\partial V}{\partial t} + m'\frac{\partial V}{\partial m} + s'_m\frac{\partial V}{\partial s_m}, \quad \mathcal{L}_z\{V\} = -rV - \kappa z\frac{\partial V}{\partial z} + \frac{1}{2}\sigma^2\frac{\partial^2 \mathrm{V}}{\partial z^2}.$$

Discretization. We define a uniform grid:

$$t^n = t_0 + n\Delta t,\ z_i,\ m_j,\ s_{m,k},\ V\left(z_i, m_j, s_{m,k}, t^n\right) \approx v^n_{ijk}.$$

Scheme. As is common in these problems (Forsyth and Labahn, 2007), we apply a standard semi-Lagrangian difference for $\frac{DV}{Dt}$:

$$\frac{DV}{Dt} \approx \frac{v^{n+1}\left(z_i, m^*_j, s^*_{m,k}\right) - v^n_{ijk}}{\Delta t},$$

where $(m^*_j, s^*_{m,k})$ are departure points interpolated from t^{n+1}. For $\mathcal{L}_z$ we use implicit finite differences

$$\mathcal{L}_z\{v^n\} \approx -rv^n_{ijk} - \kappa z_i\frac{v^n_{i+1jk} - v^n_{i-1jk}}{2\Delta z} + \frac{1}{2}\sigma^2\frac{v^n_{i+1jk} - 2v^n_{ijk} + v^n_{i-1jk}}{\Delta z^2}.$$

Control problem. The discretized version of the Hamilton–Jacobi–Bellman equation is:

$$\frac{v^n_{ijk}}{\Delta t} - \mathcal{L}_z\{v^n\} = \min_{\pi}\left[\frac{1}{\Delta t}v^{n+1}\left(z_i, m^*_j, s^*_{m,k}\right) + \lambda v_s\pi + (1-\lambda)v_sK_2\right] + mK_3.$$

At each time, the right hand side can be solved by minimizing over the set of admissible controls $\pi^n \in [0, P_{\mathrm{EV}}(t^n))$, using bilinear interpolation to calculate the value of v at the departure points. Then what remains is a set of independent standard linear systems to solve for each j and k.

Appendix F. Outcome metrics and numerical aggregation

This appendix provides formal definitions of the outcome measures used in the results section.

Consider a simulated trajectory indexed by i, with state variables $z_i(t^n), m_i(t^n), s_{m,i}(t^n)$ and policy path $\pi_i(t^n)$, defined on a discrete time grid $\{t^n\}_{n=0}^N$, with step size $\Delta t^n = t^{n+1} - t^n$.

NPV of incentive expenditures. The discounted total incentive spending is approximated by

$$\mathrm{NPV}^{(i)}_{\pi} = \int_{t_0}^{T}\pi_i(t)\,\lambda_i(t)\,v_{s,i}(t)\,e^{-r(t-t_0)}\,dt \approx \sum_{n=0}^{N-1}\pi_i(t^n)\,\lambda_i(t^n)\,v_{s,i}(t^n)\,e^{-r\left(t^n-t_0\right)}\,\Delta t^n.$$

NPV of terminal penalties. Terminal penalties on the remaining ICE stock are given by:

$$\mathrm{NPV}^{(i)}_{K_1} = m_i(T)\,K_1\,e^{-r(T-t_0)}.$$

NPV of sales penalties. Penalties applied to new ICE sales are computed as:

$$\mathrm{NPV}^{(i)}_{K_2} = \int_{t_0}^{T}\mu_{s,i}(t)\,K_2\,e^{-r(t-t_0)}\,dt \approx \sum_{n=0}^{N-1}v_{s,i}(t^n)\,\left[1-\lambda_i(t^n)\right]\,K_2\,e^{-r\left(t^n-t_0\right)}\,\Delta t^n.$$

NPV of fuel-tax revenues. Fuel-tax revenues (enter with negative sign in the government cost) are

$$\mathrm{NPV}^{(i)}_{K_3} = -\int_{t_0}^{T}m_i(t)\,K_3\,e^{-r(t-t_0)}\,dt \approx -\sum_{n=0}^{N-1}m_i(t^n)\,K_3\,e^{-r\left(t^n-t_0\right)}\,\Delta t^n.$$

Cumulative emissions. Total emissions are computed as

$$E^{(i)} = \int_{t_0}^{T}\eta\,m_i(t)\,dt \approx \eta\sum_{n=0}^{N-1}m_i(t^n)\,\Delta t^n,$$

where $\eta = 1.880$ tonnes of CO_2e per ICE vehicle per year. This calibration is based on average annual car mileage of approximately 7100 miles (UK Department for Transport, National Travel Survey, Table NTS0901, 2024 survey year) combined with the average petrol car conversion factor of 0.16450 kg CO_2e per km from the UK Government greenhouse-gas conversion factors (Department for Energy Security and Net Zero, 2024); these inputs imply approximately 1.880 tonnes per ICE vehicle per year.

For Monte Carlo experiments, each metric is computed across all simulation paths i. Reported values in the main text correspond to the median and interquartile range of the resulting empirical distributions.

Data availability

Analysis code is available from the authors on request.

References

Acemoglu, D., Aghion, P., Bursztyn, L., Hemous, D., 2012. The environment and directed technical change. Am. Econ. Rev. 102 (1), 131–166.

Aghion, P., Dechezleprêtre, A., Hemous, D., Martin, R., Van Reenen, J., 2016. Carbon taxes, path dependency, and directed technical change: evidence from the auto industry. J. Polit. Econ. 124 (1), 1–51.

Altenburg, T., Corrocher, N., Malerba, F., 2022. China's leapfrogging in electromobility. A story of green transformation driving catch-up and competitive advantage. Technol. Forecast. Soc. Change 183, 121914.

Anilan, V., Vij, A., 2024. Taking the wheel: systematic review of reviews of policies driving BEV adoption, transportation research Part D. Transp. Environ. 136, 104424.

Basei, M., Ferrari, G., Rodosthenous, N., 2024. Uncertainty over uncertainty in environmental policy adoption: Bayesian learning of unpredictable socioeconomic costs. J. Econ. Dyn. Control 161, 104841.

Bass, F.M., 1969. A new product growth for model consumer durables. Manag. Sci. 15 (5), 215–227.

Bretschger, L., Grieg, E., 2024. Carbon taxes, CO_2 emissions, and the economy: the effects of fuel taxation in the UK. Energy Policy 195, 114359.

Burnham, A., Gohlke, D., Rush, L., Stephens, T., Zhou, Y., Delucchi, M.A., Birky, A., Hunter, C., Lin, Z., Ou, S., 2021. Comprehensive Total Cost of Ownership Quantification for Vehicles with Different Size Classes and Powertrains Technical Report ANL/ESD-21/4, Argonne National Laboratory, Argonne, IL, https://doi.org/10.2172/1780970

Department for Energy Security and Net Zero, 2024. Greenhouse Gas Reporting: Conversion Factors 2024. Published 8 July 2024, last updated 30Oct2024. Accessed:. https://www.gov.uk/government/publications/greenhouse-gas-reporting-conversion-factors-2024 (31 August 2026).

Eurostat, 2025. Passenger cars per inhabitant stable in 2023. https://ec.europa.eu/eurostat/en/web/products-eurostat-news/w/ddn-20250521-1 (Accessed: 11 September 2025).

Feng, B., Ye, Q., Collins, B.J., 2019. A dynamic model of electric vehicle adoption: the role of social commerce in new transportation. Inf. Manag. 56 (2), 196–212.

Fleming, W.H., Soner, H.M., 2006. Controlled Markov Processes and Viscosity Solutions. Springer.

Flora, M., Tankov, P., 2023. Green investment and asset stranding under transition scenario uncertainty. Energy Econ. 124, 106773.

Forsyth, P.A., Labahn, G., 2007. Numerical methods for controlled Hamilton-Jacobi-Bellman PDEs in finance. J. Comput. Finance 11 (2), 1–43. https://doi.org/10.21314/JCF.2007.163

Gillingham, K., Houde, S., van Benthem, A., 2021. Consumer myopia in vehicle purchases: evidence from a natural experiment. Am. Econ. J. Econ. Policy 13 (3), 207–238.

Goodwin, P., 2020. Trends in car use, travel demand and policy thinking. In: International Transport Forum Discussion Papers, No. 2020/27. OECD Publishing, Paris, https://doi.org/10.1787/3cbb1d72-en

Goulder, L.H., 2013. Climate change policy's interactions with the tax system. Energy Econ. 40, S3–S11.

Hardman, S., Chandan, A., Tal, G., Turrentine, T., 2017. The effectiveness of financial purchase incentives for battery electric vehicles–a review of the evidence. Renew. Sustain. Energy Rev. 80, 1100–1111.

He, C., Ozturk, O.C., Gu, C., Chintagunta, P.K., 2023. Consumer tax credits for evs: some quasi-experimental evidence on consumer demand, product substitution, and carbon emissions. Manag. Sci. 69 (12), 7759–7783. https://doi.org/10.1287/mnsc.2023.4781

HM Revenue & Customs, 2026. Amended fuel duty rates: 2026 to 2027. https://www.gov.uk/government/publications/amended-fuel-duty-rates-for-2026-to-2027/amended-fuel-duty-rates-2026-to-2027 (Accessed: 31 August 2026).

INSEE, 2021. Résultats détaillés des projections de population 2021–2070 pour la France – scénario central. Insee Résultats, 29 November 2021. https://www.insee.fr/fr/statistiques/5894083.

International Energy Agency, 2024. Global EV Outlook 2024. Licence: CC BY 4.0. https://www.iea.org/reports/global-ev-outlook-2024.

International Energy Agency (IEA), 2025. Global EV data explorer. https://www.iea.org/data-and-statistics/data-tools/global-ev-data-explorer (Last updated 31 July 2025. Accessed: 1 October 2025).

Javid, R.J., Nejat, A., 2017. A comprehensive model of regional electric vehicle adoption and penetration. Transp. Policy 54, 30–42.

Légifrance, 2024. Code des impositions sur les biens et services, article L312-35: tarifs normaux des produits taxables en tant que carburant. https://www.legifrance.gouv.fr/codes/article_lc/LEGIARTI000048833665/2024-05-16 (Version in force from 1 January 2024 to 1 January 2025. Accessed: 11 September 2026).

Liao, F., Molin, E., van Wee, B., 2017. Consumer preferences for electric vehicles: a literature review. Transp. Rev. 37 (3), 252–275.

Liu, Z., Song, J., Kubal, J., Susarla, N., Knehr, K.W., Islam, E., Nelson, P., Ahmed, S., 2021. Comparing total cost of ownership of battery electric vehicles and internal combustion engine vehicles. Energy Policy 158, 112564.

Massiani, J., Gohs, A., 2015. The choice of bass model coefficients to forecast diffusion for innovative products: an empirical investigation for new automotive technologies. Res. Transp. Econ. 50, 17–28.

Meckling, J., Nahm, J., 2019. The politics of technology bans: industrial policy competition and green goals for the auto industry. Energy Policy 126, 470–479.

Metcalf, G.E., 2007. A green employment tax swap: using a carbon tax to finance payroll tax relief. Brookings Institution-World Resources Institute, Washington, DC https://www.wri.org/research/green-employment-tax-swap (Published 1 May 2007).

Mitropoulos, L.K., Prevedouros, P.D.K., 2017. Total cost of ownership and externalities of conventional, hybrid and electric vehicle. Transp. Res. Procedia 24, 267–274.

Muehlegger, E., Rapson, D.S., 2022. Subsidizing low- and middle-income adoption of electric vehicles: quasi-experimental evidence from California. J. Public Econ. 216, 104752.

OECD, 2021. Effective carbon rates 2021: pricing carbon emissions through taxes and emissions trading. In: OECD Series on Carbon Pricing and Energy Taxation. OECD Publishing, Paris, https://doi.org/10.1787/0e8e24f5-en

Office for National Statistics, 2025. National population projections: 2022-based. https://www.ons.gov.uk/peoplepopulationandcommunity/populationandmigration/populationprojections/bulletins/nationalpopulationprojections/2022based (Released 28 January 2025. Accessed: 14 April 2025).

Papke, L.E., Wooldridge, J.M., 1996. Econometric methods for fractional response variables with an application to 401(k) plan participation rates. J. Appl. Econom. 11 (6), 619–632.

Remmy, K., 2026. Adjustable product attributes, indirect network effects, and subsidy design: the case of electric vehicles. Am. Econ. J. Econ. Policy 18 (2), 107–140. https://doi.org/10.1257/pol.20230294

Rietmann, N., Hügler, B., Lieven, T., 2020. Forecasting the trajectory of electric vehicle sales and the consequences for worldwide CO_2 emissions. J. Clean. Prod. 261, 121038.

Rísquez Ramos, M., Ruiz-Gálvez, M.E., 2024. The transformation of the automotive industry toward electrification and its impact on global value chains: inter-plant competition, employment, and supply chains. European Research on Management and Business Economics 30 (1), 100242.

Service des données et études statistiques (SDES), 2025. Données sur le parc automobile français au 1ER janvier 2025. https://www.statistiques.developpement-durable.gouv.fr/donnees-sur-le-parc-automobile-francais-au-1er-janvier-2025 (Published 19 September 2025. Accessed: 11 September 2026).

Shepherd, S., Bonsall, P., Harrison, G., 2012. Factors affecting future demand for electric vehicles: a model-based study. Transp. Policy 20, 62–74.

Slowik, P., Isenstadt, A., Pierce, L., Searle, S., 2022. Assessment of light-duty electric vehicle costs and consumer benefits in the United States in the 2022–2035 time frame. White paper, International Council on Clean Transportation, 18 October 2022. https://theicct.org/publication/ev-cost-benefits-2035-oct22/.

Springel, K., 2021. Network externality and subsidy structure in two-sided markets: evidence from electric vehicle incentives. Am. Econ. J. Econ. Policy 13 (4), 393–432.

Sterner, T., 2007. Fuel taxes: an important instrument for climate policy. Energy Policy 35 (6), 3194–3202.

Szabó, D.Z., Csóka, P., Janosik, R., 2025. The optimal timing of clean technology adoption: a stochastic cost–benefit analysis. Technol. Forecast. Soc. Change 219, 124276.

van Dender, K., Clever, M., 2013. Recent trends in car usage in advanced economies – slower growth ahead? Summary and conclusions. In: International Transport Forum Discussion Papers, No. 2013/09. OECD Publishing, Paris, https://doi.org/10.1787/5k46n4121k5d-en

Xing, J., Leard, B., Li, S., 2021. What does an electric vehicle replace? J. Environ. Econ. Manag. 107, 102432.